

# Noncovalent interactions from models for the Møller-Plesset adiabatic connection

Timothy J. Daas,<sup>†</sup> Eduardo Fabiano,<sup>‡,P</sup> Fabio Della Sala,<sup>‡,P</sup> Paola Gori-Giorgi,<sup>†</sup>  
and Stefan Vuckovic<sup>\*,§,||,†</sup>

<sup>†</sup>*Department of Chemistry & Pharmaceutical Sciences and Amsterdam Institute of  
Molecular and Life Sciences (AIMMS), Faculty of Science, Vrije Universiteit, De Boelelaan  
1083, 1081HV Amsterdam, The Netherlands*

<sup>‡</sup>*Institute for Microelectronics and Microsystems (CNR-IMM), Via Monteroni, Campus  
Unisalento, 73100 Lecce, Italy*

<sup>P</sup>*Center for Biomolecular Nanotechnologies, Istituto Italiano di Tecnologia, Via Barsanti  
14, 73010 Arnesano (LE), Italy*

<sup>§</sup>*Physical and Theoretical Chemistry, University of Saarland, 66123 Saarbrücken, Germany*

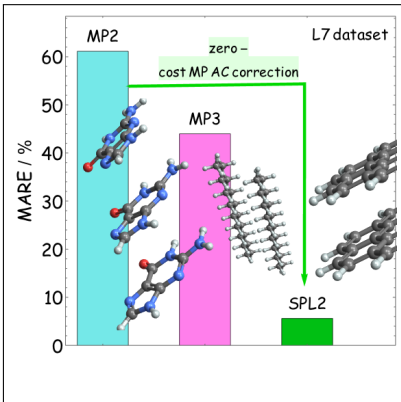
<sup>||</sup>*Department of Chemistry, University of California, Irvine, CA 92697, USA*

E-mail: svuckovi@uci.edu

## Abstract

Given the omnipresence of non-covalent interactions (NCIs), their accurate simulations are of crucial importance across various scientific disciplines. Here we construct accurate models for the description of NCIs by an interpolation along the Møller-Plesset adiabatic connection (MP AC). Our interpolation approximates the correlation energy, by recovering MP2 at small coupling strengths and the correct large-coupling strength expansion of the MP AC, recently shown to be a functional of the Hartree-Fock density. Our models are size consistent for fragments with non-degenerate ground states, have the same cost as double hybrids and require no dispersion corrections to capture NCIs accurately. These interpolations greatly reduce large MP2 errors for typical  $\pi$ -stacking complexes (e.g., benzene-pyridine dimers) and for the L7 dataset. They are also competitive with state-of-the-art dispersion enhanced functionals and can even significantly outperform them for a variety of datasets, such as CT7 and L7.

## Graphical TOC Entry



An accurate description of noncovalent interactions (NCIs) is crucial for fields ranging from chemistry, biology and materials science, with a plethora of methods being constantly developed, tested and improved.<sup>1–19</sup> Second-order Møller-Plesset (MP2) perturbation theory has been often considered a relatively safe choice for the treatment of NCIs in chemistry, given its favorable scaling relative to more sophisticated wave-function methods and encouraging early successes in capturing NCIs in small systems.<sup>20,21</sup> The described failures of MP2 when applied to NCIs, such as those in stacking complexes, have been often considered accidental. Very recently, Furche and co-workers<sup>22</sup> have shown that MP2 relative errors for NCIs can grow systematically with molecular size, and that the whole MP series may be even qualitatively unsuitable for the description of large non-covalent complexes. On the other hand, double hybrid (DH) functionals, that mix density-functional theory (DFT) semilocal ingredients with a fraction of Hartree-Fock (HF) exchange and MP2 correlation energy, typically worsen the performance of MP2 for NCIs,<sup>23–25</sup> unless dispersion corrections are added on top of them.<sup>12,26,27</sup> A few notable exceptions to this are the XYGn family of functionals<sup>28,29</sup> and recent DHs developed in Martin’s group,<sup>30</sup> which give accuracy improvements over MP2 without requiring additional dispersion corrections.

In this work, we use an adiabatic connection (AC) formalism in which the MP series arises in the weak-coupling limit (hereinafter MP AC) to construct a correction to the MP2 interaction energies, which is guaranteed to be size consistent for the case in which the fragments have a non-degenerate ground-state. We construct this correction using two different strategies both based on an interpolation between MP2 and the strong-coupling limit of the MP AC, which has been recently studied in detail,<sup>31,32</sup> and shown to be given by functionals of the Hartree-Fock (HF) density with a clear physical meaning. The resulting method gives major improvements over MP2, despite coming at a negligible extra computational cost. In Fig. 1 we show, in particular, that a specific interpolation form named ‘SPL2’ – an extension of the approach of Seidl, Perdew and Levy<sup>33</sup> (SPL) – is competitive with state-of-the art electronic structure methods when applied to the challenging L7 dataset.<sup>22,34–36</sup> In what fol-

lows, we will describe the theoretical basis for the construction of this new class of functionals based on the MP AC interpolation. We also introduce and analyse the different interpolation schemes within this framework and discuss possible routes to further refinement.

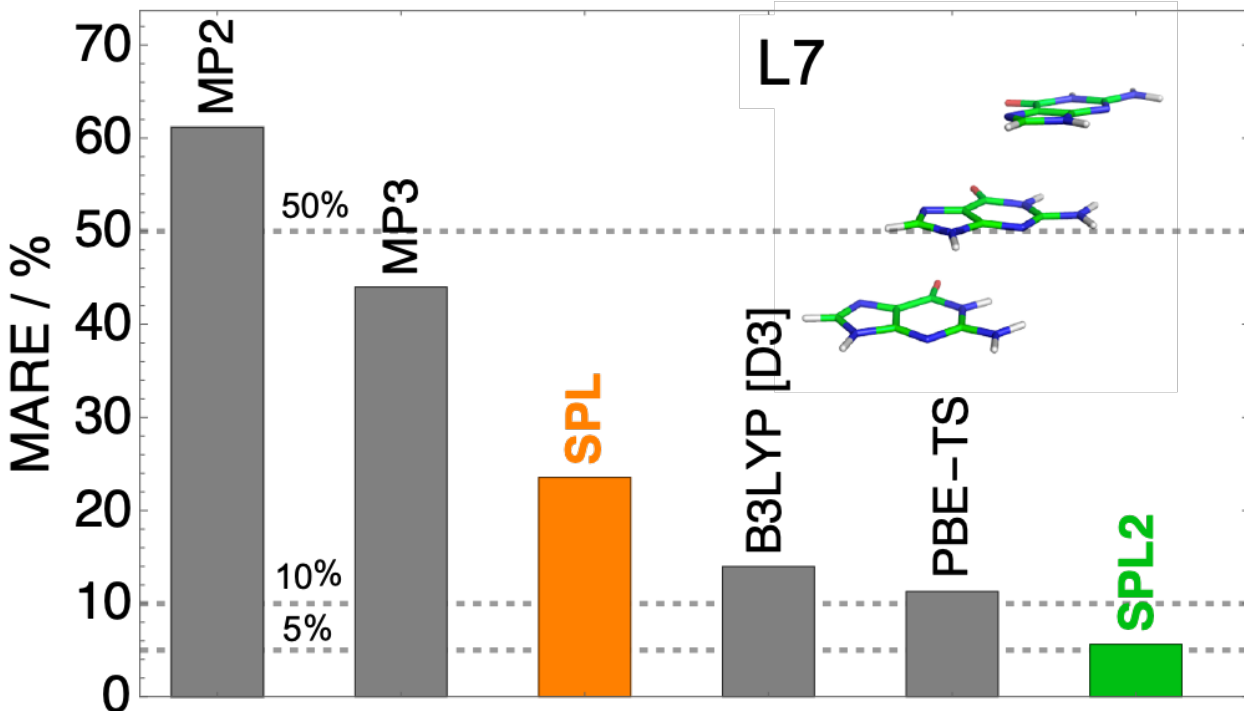


Figure 1: The mean absolute relative errors (MARE) for selected methods, where TS stands for the Tkatchenko-Shefler method,<sup>37</sup> for the L7 dataset using the reference data of Grimme and co-workers.<sup>36</sup>

*Theory-* For the construction of our approximations, we use the Møller-Plesset adiabatic connection (MP AC) framework, whose hamiltonian reads as:

$$\hat{H}_\lambda = \hat{T} + \hat{V}_{\text{ext}} + \lambda \hat{V}_{ee} + (1 - \lambda) (\hat{J} + \hat{K}), \quad (1)$$

with  $\hat{T}$  the kinetic energy,  $\hat{V}_{ee}$  the electron-electron repulsion operators. Here  $\hat{J} = \hat{J}[\rho^{\text{HF}}]$  and  $\hat{K} = \hat{K}[\{\phi_i^{\text{HF}}\}]$  are the standard Hartree-Fock (HF) Coulomb and exchange operators in terms of the HF density  $\rho^{\text{HF}}$  and the occupied orbitals  $\phi_i^{\text{HF}}$ , respectively. We denote with  $\Psi_\lambda$  the ground-state of  $\hat{H}_\lambda$ , which at  $\lambda = 1$  corresponds to the physical system and at  $\lambda = 0$  to the HF Slater determinant. In terms of these quantities the traditional quantum-chemical

definition of the correlation energy is given by

$$E_c = \langle \Psi | \hat{H} | \Psi \rangle - \langle \Psi_0 | \hat{H} | \Psi_0 \rangle, \quad (2)$$

with  $\hat{H} = \hat{H}_{\lambda=1}$  and  $\Psi = \Psi_{\lambda=1}$ . Applying the Hellman–Feynman theorem to Eq. (1), one obtains the AC expression for the correlation energy, which reads as<sup>22,31,32,38,39</sup>

$$E_c = \int_0^1 W_{c,\lambda} d\lambda, \quad (3)$$

where  $W_{c,\lambda}$  is the AC integrand,

$$W_{c,\lambda} = \langle \Psi_\lambda | \hat{V}_{ee} - \hat{J} - \hat{K} | \Psi_\lambda \rangle - \langle \Psi_0 | \hat{V}_{ee} - \hat{J} - \hat{K} | \Psi_0 \rangle. \quad (4)$$

The small  $\lambda$  expansion of  $W_{c,\lambda}$  returns the Møller-Plesset (MP) series:

$$W_{c,\lambda \rightarrow 0} = \sum_{n=2}^{\infty} n E_c^{\text{MP}n} \lambda^{n-1}, \quad (5)$$

where  $E_c^{\text{MP}n}$  is the  $n$ -th order correlation energy from the MP perturbation theory.<sup>31,40</sup> Very recently, the large- $\lambda$  expansion of  $W_{c,\lambda}$  has been shown to have the following form:<sup>32</sup>

$$W_{c,\lambda \rightarrow \infty} = W_{c,\infty} + \frac{W_{\frac{1}{2}}}{\sqrt{\lambda}} + \frac{W_{\frac{3}{4}}}{\lambda^{\frac{3}{4}}} + \dots, \quad (6)$$

which is analogous, although with important differences, to the one appearing in the density fixed DFT adiabatic connection (DFT AC).<sup>31,41,42</sup> In the DFT AC the correlation energy is given by<sup>43,44</sup>

$$\begin{aligned} E_c^{\text{DFT}}[\rho] &= \langle \Psi | \hat{H} | \Psi \rangle - \langle \Psi_0^{\text{DFT}} | \hat{H} | \Psi_0^{\text{DFT}} \rangle \\ &= \int_0^1 W_{c,\lambda}^{\text{DFT}} d\lambda, \end{aligned} \quad (7)$$

where  $\Psi_\lambda^{\text{DFT}}$  integrates to the physical density  $\rho$  and minimizes the sum of  $\hat{T} + \lambda \hat{V}_{ee}$ . Defined this way,  $\Psi_\lambda^{\text{DFT}}$  is in general equal to  $\Psi_\lambda$  only at  $\lambda = 1$ . Furthermore, the density of  $\Psi_\lambda$  varies with  $\lambda$ , whereas the density of  $\Psi_\lambda^{\text{DFT}}$  is always the same by construction. The DFT AC integrand  $W_{c,\lambda}^{\text{DFT}}$  reads as:

$$W_{c,\lambda}^{\text{DFT}} = \langle \Psi_\lambda^{\text{DFT}} | \hat{V}_{ee} | \Psi_\lambda^{\text{DFT}} \rangle - \langle \Psi_0^{\text{DFT}} | \hat{V}_{ee} | \Psi_0^{\text{DFT}} \rangle. \quad (8)$$

In the following relations we will also make use of  $W_\lambda^{\text{DFT}}$ , defined to include the exchange energy:  $W_\lambda^{\text{DFT}} = W_{c,\lambda}^{\text{DFT}} + E_x$ . The functional  $W_{c,\lambda}^{\text{DFT}}$  has large<sup>45–47</sup> and small  $\lambda$ <sup>48,49</sup> expansions analogous (but not identical) to those given by Eqs. (5) and (6). The large- $\lambda$  limits of the two integrands are related by:<sup>31</sup>

$$W_{c,\infty}[\rho^{\text{HF}}] = W_\infty^{\text{DFT}}[\rho^{\text{HF}}] + \beta[\rho^{\text{HF}}]E_x[\{\phi_i^{\text{HF}}\}], \quad (9)$$

where dimensionless  $\beta[\rho^{\text{HF}}]$  is system-dependent, known to satisfy<sup>31</sup>  $\beta[\rho^{\text{HF}}] \geq 1$ , and for the uniform electron gas (UEG) it is exactly equal to 1.<sup>32</sup> By linking  $W_{c,\infty}$  and  $W_\infty^{\text{DFT}}$  and by knowing some exact features of  $\beta[\rho^{\text{HF}}]$ , Eq. (9) will be used in this work for building approximations to  $W_{c,\infty}$ , exploiting the existing approximations for its DFT counterpart.<sup>50–54</sup>

*Building approximations-* The AC framework has always played a crucial role in the construction of DFT approximations,<sup>28,55–61</sup> and, more recently, also in wave function theories, to approximate missing parts of the correlation energy (see, e.g., the work of Pernal and co-workers<sup>62,63</sup>). In the present work, we build upon the interaction strength interpolation (ISI) idea of Seidl and co-workers,<sup>33,64</sup> in which the DFT correlation energy is approximated by interpolating the AC integrand between its weak- and strong-coupling expansions. This construction enables one to include more pieces of information into the approximate correlation energy, avoiding a bias towards the weak correlation regime, present in most of the DFT approximations.<sup>33,53,61,64,65</sup> The lack of size-consistency of the ISI approach had been considered its main drawback, but a recent remarkably simple size-consistency correction (SCC)

fixes this problem in an exact way, at least for systems dissociating into fragments with a non-degenerate ground state.<sup>23,66</sup> This SCC has been used for building functionals<sup>23,66,67</sup> in the DFT context, and has been already shown to be crucial for the accuracy of model MP AC curves (see Section S3 of Ref. 66) that can signal when an MP2 calculation is not reliable.<sup>66</sup>

The idea of this work is to use this approach, originally designed for the DFT AC, in the MP AC context to build accurate approximations to describe NCIs. The mentioned SCC<sup>23</sup> is also used throughout this work to restore size-consistency of our MP AC models.

In a previous work on NCI's,<sup>23</sup> the ISI idea has been applied within the DFT AC framework, by using MP2 as an approximation for the small- $\lambda$  expansion of the DFT AC. The interpolation function used was the one developed in the DFT AC framework by Seidl, Perdew and Levy (SPL),<sup>33</sup>

$$W_{c,\lambda}^{\text{SPL}} = W_{c,\infty} \left( 1 - \frac{1}{\sqrt{1 + b\lambda}} \right), \quad (10)$$

where  $b = (4E_c^{\text{MP2}}) / W_{c,\infty}$ . Such an attempt could be also viewed as an interpolation model for the MP AC in which the large- $\lambda$  limit was approximated by its DFT counterpart  $W_{c,\infty}^{\text{DFT}}$ , which is known to be accurately described<sup>41,68</sup> by the point-charge plus continuum (PC) model<sup>50</sup>

$$\begin{aligned} W_{c,\infty}[\rho^{\text{HF}}] &\sim W_{c,\infty}^{\text{DFT}}[\rho^{\text{HF}}] \\ &\approx \underbrace{\int \left[ A\rho^{\text{HF}}(\mathbf{r})^{4/3} + B \frac{|\nabla \rho^{\text{HF}}(\mathbf{r})|^2}{\rho^{\text{HF}}(\mathbf{r})^{4/3}} \right] d\mathbf{r}}_{W_{\infty}^{\text{PC}}[\rho^{\text{HF}}]} \\ &\quad - E_x[\{\phi_i^{\text{HF}}\}], \end{aligned} \quad (11)$$

where  $A = -1.451$ ,  $B = 5.317 \times 10^{-3}$ . Notice that this approximation is not in line

with the exact relation of Eq. (9), which was not known at the time, but it can still provide reasonable results. By performing a simple MP2 calculation and evaluating  $W_{c,\infty}$  on the HF density, the needed quantities to be fed into Eq. (10) were easily obtained, yielding<sup>23,66</sup> the SPL approximation to  $E_c$  (Eq. 3). When it comes to NCIs, SPL was found<sup>23,66</sup> to give a major improvement over MP2 (see Fig. 2). However, the deficiencies of SPL for NCIs are also already noticeable in Fig. 2, where we show results for various NCI’s data sets. On the  $x$ -

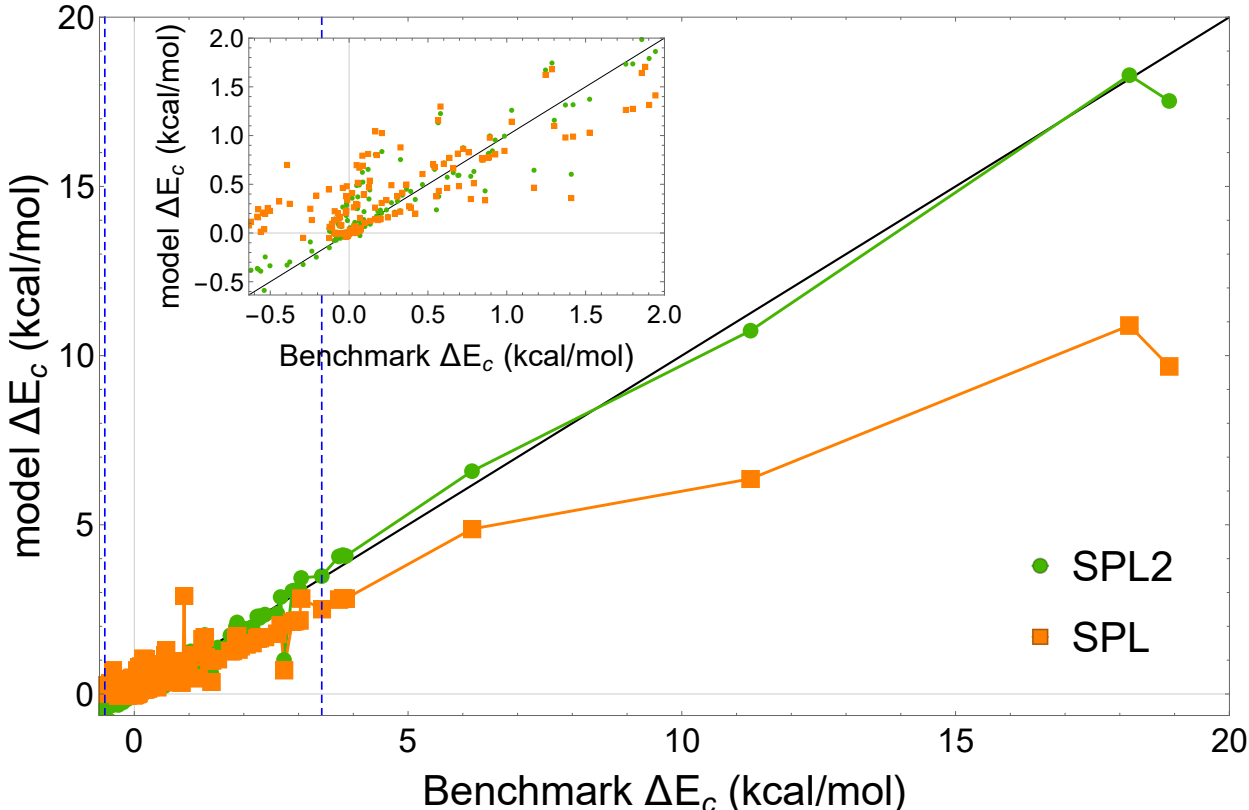


Figure 2: Difference between benchmark CCSD(T) correlation energies and those of MP2 ( $\Delta E_c = E_c - E_c^{\text{MP2}}$ ) vs  $\Delta E_c$  predicted by our models for a range of interaction energies of the NCI complexes [S22, S66, DI6, CT7, NGD8 and L7 datasets]. The blue vertical dashed lines denote the range in which  $\Delta E_c$  values of complexes in S22, the dataset we used to train empirical parameters in the SPL2 form, lie.

axis, we report the difference between the benchmark CCSD(T) and MP2 correlation energy  $\Delta E_c = E_c - E_c^{\text{MP2}}$ , and the difference between the benchmark and SPL correlation energies is reported on the  $y$ -axis. This way, if SPL had the same level of accuracy as the benchmark, all data points would lie on the  $y = x$  line (shown in black). The plotted correlation energies



pertain to the interaction energies, i.e. the differences between correlation energies of a complex and its fragments. Since MP2 (with large enough basis set) overbinds most of the complexes,<sup>66,69</sup>  $\Delta E_c$  is positive for most of the datapoints. We can see from the same figure that SPL decently corrects MP2 for different ranges of  $\Delta E_c$ . As  $\Delta E_c$  becomes large, SPL still substantially reduces the error of MP2. But, the performance of SPL is still not satisfactory as even the reduced errors can easily exceed 5 kcal/mol. Moreover, for few systems where MP2 underbinds, SPL corrects it in the wrong direction (see the inset of Fig. 2 that zooms in on the region around  $\Delta E_c=0$ ). In these cases, a model MP AC integrand should be concave to correct the underbinding of MP2, and the SPL model is not flexible enough to always capture this concavity.<sup>66</sup>

From these examples, it is clear that we need better interpolation forms than SPL to model  $W_{c,\lambda}$ , and a better description of its  $\lambda \rightarrow \infty$  limit, which is known to be different<sup>31,32</sup> than the DFT one used in this SPL construction. To make the interpolation form more flexible in capturing the concavity/convexity correctly when MP2 underbinds/overbinds, respectively, we consider a form containing two SPL terms:

$$W_{c,\lambda}^{\text{SPL2}} = C_1 - \frac{m_1}{\sqrt{1+b_1\lambda}} - \frac{m_2}{\sqrt{1+b_2\lambda}}. \quad (12)$$

We call this form SPL2, with the  $b_1$ ,  $m_1$  and  $C_1$  parameters fixed by the exact conditions: i)  $W_{c,\lambda}^{\text{SPL2}}$  vanishes at 0, ii) its initial derivative is equal to  $2E_c^{\text{MP2}}$  (Eq. 5), and iii) it converges to  $W_{c,\infty}$  in the large  $\lambda$  limit (Eq. 6),

$$\begin{aligned} C_1 &= W_{c,\infty}^{\alpha\beta}; \\ b_1 &= \frac{b_2 m_2 - 4E_c^{\text{MP2}}}{m_2 - W_{c,\infty}^{\alpha\beta}}; \\ m_1 &= W_{c,\infty}^{\alpha\beta} - m_2, \end{aligned} \quad (13)$$

where  $W_{c,\infty}^{\alpha\beta}[\rho^{\text{HF}}]$  is an approximation to  $W_{c,\infty}[\rho^{\text{HF}}]$  inspired by Eq. (9):

$$W_{c,\infty}^{\alpha\beta}[\rho^{\text{HF}}] = \alpha W_{\infty}^{\text{PC}}[\rho^{\text{HF}}] + \beta E_x[\{\phi_i^{\text{HF}}\}]. \quad (14)$$

In fact, as mentioned, the exact form of  $W_{c,\infty}$  for the MP AC has been recently revealed,<sup>31,32</sup> but it is quite involved, with targeted semilocal approximations still under construction; the use of Eq. (9) to improve the large- $\lambda$  description of the MP AC seems a rather effective first step. There are now 4 parameters left in the SPL2 model for MP AC ( $b_2$ ,  $m_2$ ,  $\alpha$ , and  $\beta$  that we simplify to be system independent), which we fit in this work to the S22 dataset<sup>70,71</sup> by minimizing its mean absolute error (MAE). From Fig. 2, we can see that SPL2 fixes the key deficiencies of SPL: it corrects MP2 in the right direction when the latter underbinds, and has a better corrective trend than SPL as MP2 errors become large.

In addition to the SPL2 model, we also develop a model for  $E_c$  directly. We first generalize  $E_c$  as:  $E_{c,\lambda} = \int_0^\lambda W_{c,\lambda'} d\lambda'$ , such that  $E_c = E_{c,\lambda=1}$ . Then we build the following model for  $E_{c,\lambda}$ :

$$E_{c,\lambda}^{\text{MPACF-1}} = -g\lambda + \frac{g(h+1)\lambda}{\sqrt{d_1^2\lambda+1} + h\sqrt[4]{d_2^4\lambda+1}}, \quad (15)$$

with

$$\begin{aligned} g &= -W_{c,\infty}^{1,1} \\ h &= \frac{4E_c^{\text{MP2}} - 2d_1^2W_{c,\infty}^{1,1}}{-4E_c^{\text{MP2}} + d_2^4W_{c,\infty}^{1,1}}, \end{aligned} \quad (16)$$

where  $W_{c,\infty}^{1,1}$  is  $W_{c,\infty}^{\alpha\beta}$  in which  $\alpha$  and  $\beta$  are set to 1 by using the UEG argument (see above). This new model is called Møller-Plesset Adiabatic Connection Functional-1 (MPACF-1) and will be the starting point for a new class of functionals that approximate the MPAC. The underlying MP AC model,  $W_{c,\lambda}^{\text{MPACF-1}}$ , is simply obtained by taking a derivative of  $E_{c,\lambda}^{\text{MPACF-1}}$  w.r.t.  $\lambda$ . In contrast to  $W_{c,\lambda}^{\text{SPL}}$  and  $W_{c,\lambda}^{\text{SPL2}}$ ,  $W_{c,\lambda}^{\text{MPACF-1}}$  contains the  $W_{\frac{3}{4}}$  term appearing in the large  $\lambda$  limit (Eq. 6), making this model having a better asymptotic behavior than SPL

and SPL2. MPACF-1 is also less empirical than SPL2 since it contains only two parameters ( $d_1$  and  $d_2$ ), which we again fit to the S22 datasets and report their optimal values in the Computational Details below.

Without the SCC, SPL2 and MPACF-1 have a different size-extensivity behaviour. Nevertheless, in this work we always use the SCC ensuring that the interaction energies are correctly computed and vanish in the dissociation limit (see Fig. S1 from the Supplementary Information<sup>72</sup> for the  $\text{Kr}_2$  example and the caption of this figure for a further discussion). From Fig. S1, one can also see that the SCC does not affect the shape of the potential energy surfaces (PES), but only shifts a PES by a constant ensuring that binding energies vanish when the fragments are infinitely away from one another. Thus, the SCC would not be required and has no effect for calculating differences in energies at different stationary points of a PES (e.g. reaction energies, barrier heights, isomerisation energies, etc).

In what follows, we compare the performance of SPL2 and MPACF-1 with that of earlier SPL, MP2 and other approximations for NCIs. While our models share some similarities with DHs, there are two key differences. First, our models are based on the full amounts of the exact exchange and MP2 correlation and thus they do not benefit from error cancellations between these quantities and their semilocal counterparts. Furthermore, our models do not require dispersion corrections to be accurate for NCIs.

*Results-* We start with a light example, showing the  $\text{Kr}_2$  binding curve in Fig. 3. We can see from the top panel of Fig. 3 that SPL significantly improves MP2. At the same time, SPL is significantly improved by MPACF-1 and SPL2, with the latter being slightly more accurate than the former. This happens even though noble gas dimers are beyond our training set (S22). In contrast, the D3 empirical correction can even worsen binding curves of noble gas dimers,<sup>73</sup> even though their binding energies have been used in the training of the original D3 parameters.<sup>12</sup> Now we move to the bottom panel of Fig. 3, where we look at the accuracy of different AC models for the interaction energies for  $\text{Kr}_2$  at equilibrium. To test the accuracy of our AC models, we need a reference  $W_{c,\lambda}$  for the interaction energies. Ideally,

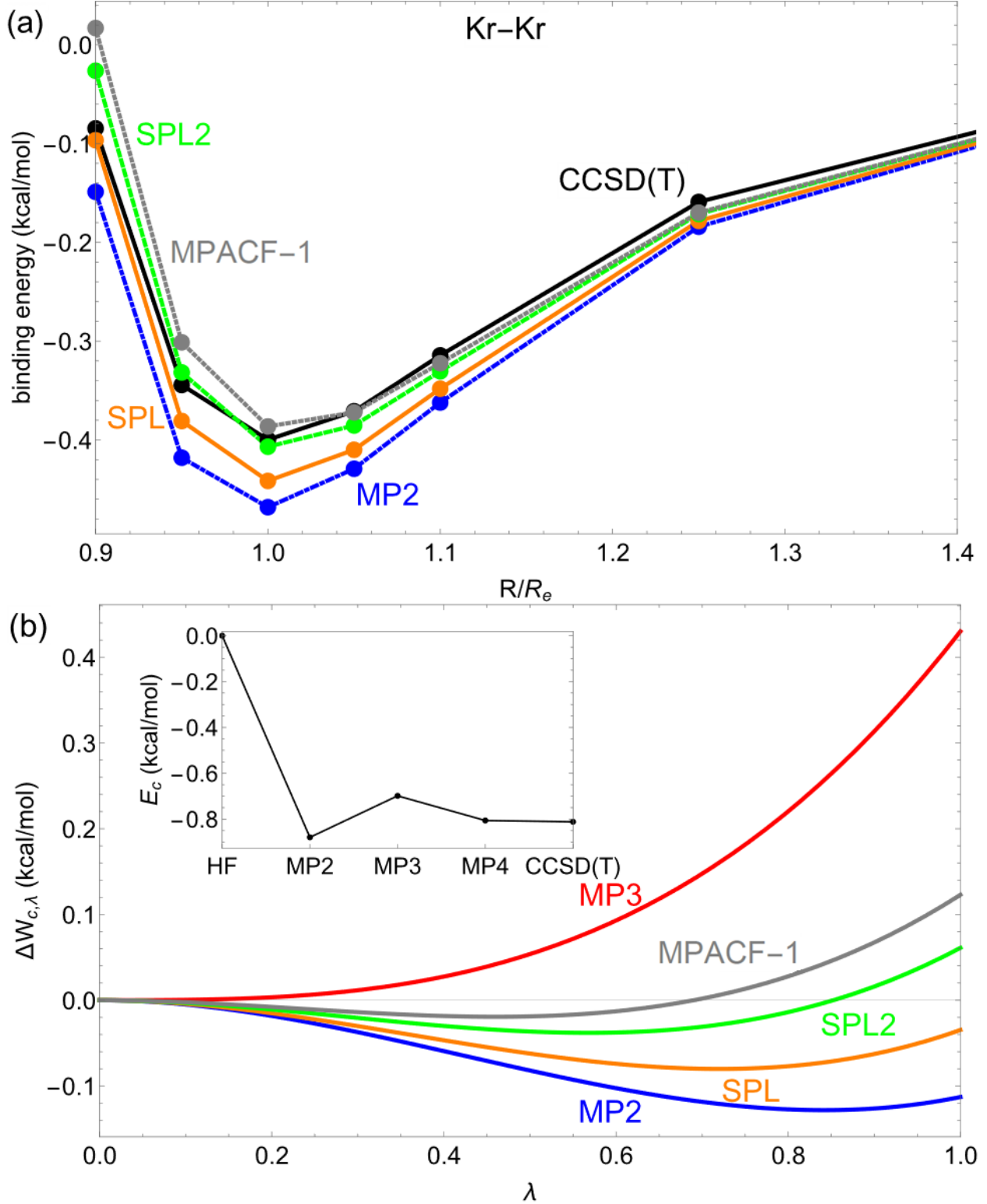


Figure 3: Panel (a): The interaction energies of MP2, SPL, SPL2 and MPACF-1 as well as reference CCSD(T) curves for Kr<sub>2</sub>. Panel (b): The errors of different MP AC models for Kr<sub>2</sub> at equilibrium,  $\Delta W_{c,\lambda} = W_{c,\lambda}^{\text{method}} - W_{c,\lambda}^{\text{ref}}$ , where the r.h.s. of Eq 5 truncated to fourth order,  $W_{c,\lambda}^{\text{MP4}}$ , is taken as a reference (the inset justifies this choice given the (fast) convergence of MP $n$  series).

this quantity would be obtained by full-CI or CCSD(T), but we note that the convergence of  $MPn$  series for the interaction energy of  $Kr_2$  at equilibrium is fast (see the inset of the lower panel of Fig. 3 showing that MP4 gives nearly the same results as CCSD(T)). For this reason, we can safely assume that the r.h.s. of Eq. (5) truncated to fourth order gives us a reliable MP AC reference for the interaction energies of  $Kr_2$ . After establishing  $W_{c,\lambda}^{MP4}$  as a reference, we compare the performance of MP3, MP2, SPL, SPL2 and MPACF-1 curves in the lower panel of Fig. 3). The error of all MP AC models slowly increases as we move away from  $\lambda = 0$  since all the curves have the correct initial slope given by  $2E_c^{MP2}$ . On average, SPL2 is the most accurate. MPACF-1 is the most accurate up to  $\lambda \sim 0.7$ , then its accuracy deteriorates and at about  $\lambda \sim 0.9$  where it is less accurate than even SPL. Overall, all three AC models give significant improvements over MP2 and MP3.

**Table 1: The MAE in kcal/mol of different methods for the S22, CT7, DI6, S66 and L7 datasets from the existing literature. Best results are highlighted in bold. NGD8 is a set of 8 noble gas dimers ( $Ar_2$ ,  $He_2$ ,  $Kr_2$ ,  $Ne_2$ ,  $ArKr$ ,  $C_6H_6-Ne$ ,  $CH_4Ne$  and  $HeAr$ ) that we construct here.**

set	MP2	SPL	SPL2	MPACF-1	B3LYP-D3
NGD8	0.04	0.05	<b>0.03</b>	<b>0.03</b>	0.08
CT7	0.92	0.57	<b>0.45</b>	0.60	1.48
DI6	0.48	0.27	<b>0.18</b>	0.20	0.46
S22	0.88	0.38	<b>0.15</b>	0.19	<b>0.15</b>
S66	0.47	0.35	0.21	0.26	<b>0.18</b>
L7	8.74	3.83	<b>0.89</b>	2.32	1.78

Now we move to Table 1, where we show the results for several datasets<sup>34,69,70,74–76</sup> in comparison with the B3LYP hybrid enhanced by D3. Except for noble gas dimers where the differences in MAEs are marginal, SPL improves the performance of MP2 by a factor of 2 on average. SPL2 greatly improves SPL by reducing its errors by the factors ranging from 1.3 (CT7) to more than 4 (L7). MPACF-1 provides still a substantial improvement over SPL, but on average performs worse than SPL2. SPL2 also beats B3LYP-D3 for NGD8, CT7, DI6 and L7, whereas the two approaches display a similar performance for S22 and S66. By looking at MAEs for individual subsets of the S66 dataset (see Table S1 from the

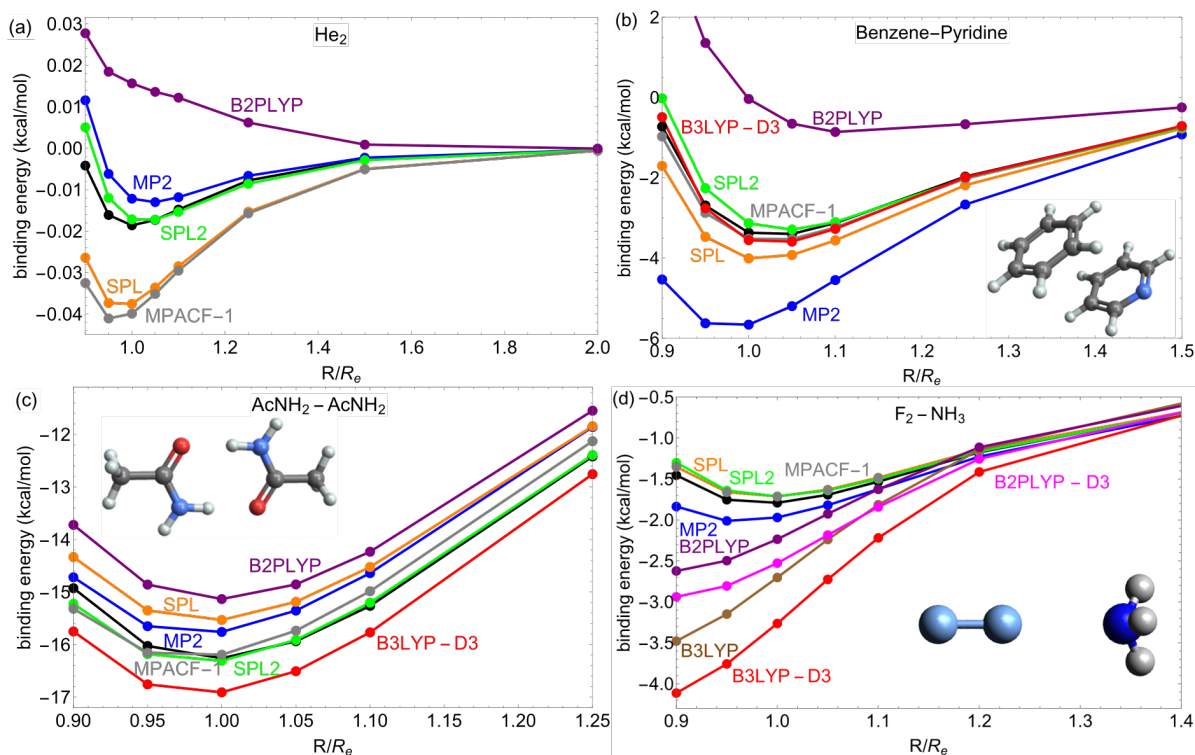


Figure 4: Dissociation curves of  $\text{He}_2$  (a), benzene-pyridine (b), acetamide (c), and  $\text{NH}_3$ - $\text{F}_2$  dimers (d), obtained from various methods. CCSD(T) (black line) has been used as a reference for all complexes. For other binding curves, see Figs. S3-S8 from the Supplementary Information.<sup>72</sup>

Supplementary Information<sup>72</sup>), we can see that the accuracy of MP2 is high for hydrogen bonded complexes, but it is well-known that it deteriorates for dispersion-bonded and mixed complexes.<sup>66,69</sup> SPL greatly reduces the errors of MP2 for dispersion-bonded and mixed complexes, but becomes worse than MP2 for hydrogen bonds. On the other hand, SPL2 greatly improves MP2 for dispersion-bonded and mixed complexes, without deteriorating its accuracy for hydrogen bonds.

In Fig. 4, we show several binding curves representing NCIs of different nature. This includes weakly-bonded  $\text{He}_2$  [panel (a)], stacked Benzene-Pyridine complex [panel (b)], hydrogen-bonded acetamide dimer [panel (c)], and the charged-transfer (CT) fluorine-ammonia complex [panel (d)]. Overall, SPL2 is in the closest agreement with the reference [CCSD(T)] and it corrects MP2 in the right direction in cases when MP2 underbinds ( $\text{He}_2$ , the acetamide dimer), when it overbinds slightly (the fluorine-ammonia complex), and severely (the benzene-pyridine complex). On the other hand, SPL corrects MP2 in the right direction only in cases when the latter overbinds. MPACF-1 is off for  $\text{He}_2$ , but in other cases it is on par with SPL2 and even more accurate than SPL2 in the case of the benzene-pyridine dimer. For  $\text{He}_2$ , SPL is as bad as MPACF-1, whereas empirical SPL2 is very accurate (even though noble gases have not been used in the training of SPL2). Thus, it seems indeed challenging to build non-empirical MP AC model that will give improvements over MP2 for  $\text{He}_2$ , but may be achieved in the future by considering approximations to higher-order terms from the large  $\lambda$  limit of the MP AC.<sup>32</sup>

Our models are accurate for NCIs without requiring dispersion corrections (in contrast to e.g., D3-uncorrected B2PLYP, which is off for all four cases). B3LYP corrected by D3 is completely off for  $\text{He}_2$  (see Fig. S3 from the Supplementary Information<sup>72</sup>). The behavior of B3LYP and B2PLYP is even more interesting in the case of the CT fluorine-ammonia complex where the D3 correction even worsens the original results.<sup>77</sup> This is not due to the D3 correction itself, but due to the density-driven errors that typically bedevil semilocal DFT calculations of halogen-based CT complexes<sup>78–80</sup> (Note also that is not uncommon that the

D3 correction worsens the results from semilocal DFT calculations suffering from density-driven errors<sup>78,79</sup>). On the contrary, our MP AC models are built only for correlation, and thus the full amount of the exact exchange is used without being mixed with a fraction of its semilocal counterpart. This is probably the reason why all of our MP AC models are very accurate for the studied CT complex (see also Fig. S7 from the Supplementary Information<sup>72</sup> for another example).

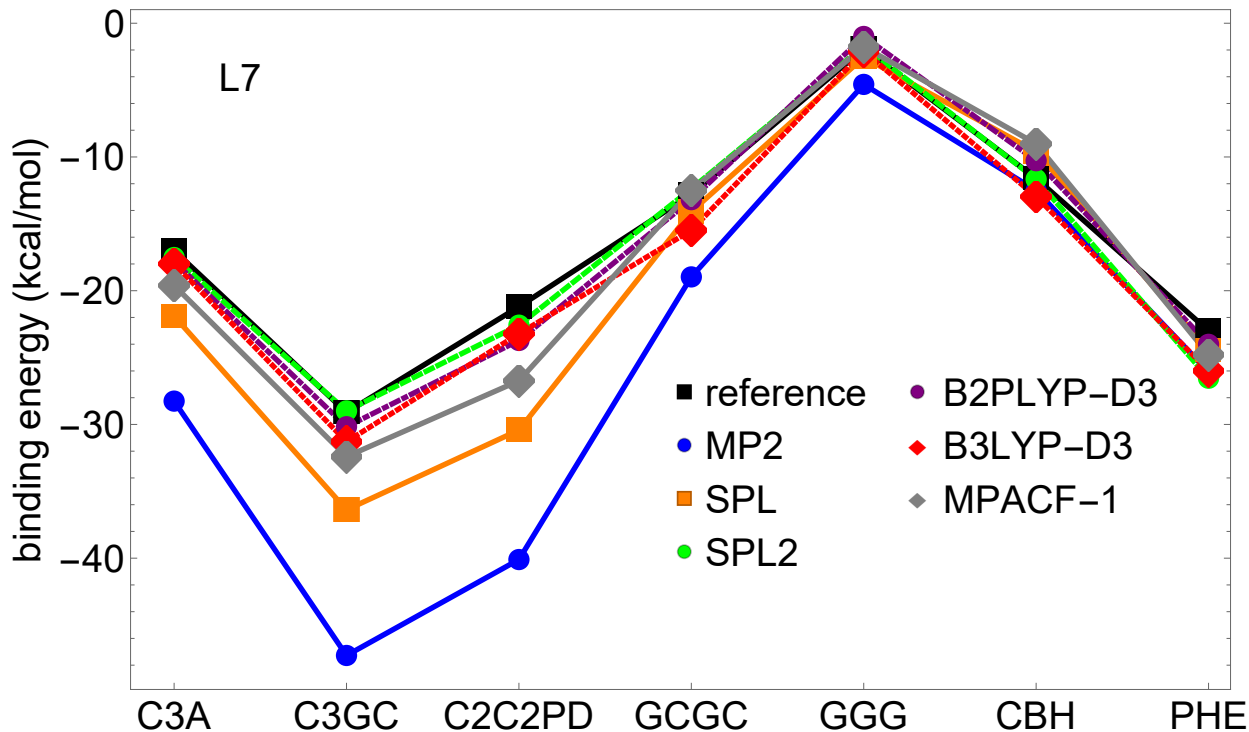


Figure 5: Interaction energies of MP2, SPL, SPL2, B3LYP-D3 and B2PLYP as well as reference data of Grimme and co-workers,<sup>36</sup> plotted for individual complexes of the L7 dataset. For comparison of the approximations against other reference data, see Fig. S2 and Table S2 from the Supplementary Information.<sup>72</sup>

Now we go back to the L7 dataset composed by larger complexes for which MP2 displays very large errors.<sup>22</sup> Interaction energies for individual L7 complexes are shown in Fig. 5, where the reference used is obtained from Grimme et al.<sup>36</sup> From Fig. 5, we can see that MP2 strongly overbinds most the L7 complexes. SPL corrects it, but not sufficiently, as it is still much less accurate than B3LYP-D3 and B2PLYP-D3. MPACF-1 improves SPL, but a better performance is obtained from our SPL2 model, which very accurately reproduces the



reference values. In the SI (Table S2 and Fig. S2 from the Supplementary Information<sup>72</sup>), we compare the performance of our models against other L7 references from the literature.<sup>34,35</sup> From these results, it can be seen that regardless of what reference is used, SPL greatly reduces the MP2 errors, whereas our new models (SPL2 and MPACF-1) greatly reduce the errors of SPL.

*Conclusions and Perspectives* – In summary, we have introduced a new scheme for the construction of MP AC models providing accurate description of NCIs. Two specific interpolation models, SPL2 and MPACF-1 greatly reduce errors of MP2 and earlier proposed SPL for a variety of NCIs despite coming at a negligible computational cost beyond that of MP2. In comparison with e.g. modern (double) hybrids,<sup>81–83</sup> empirical parameters in our models have been primitively optimized and despite that offer highly competitive accuracy for the description of NCIs. Further improvements can be obtained by better optimization strategies, but also by reducing empiricism using the additional recently revealed exact form of the large  $\lambda$  limit MP AC functionals.<sup>32</sup> Furthermore, one can use machine learning to find improved ways for interpolating MP AC (see, e.g. Ref 84 for a related work). To lower the cost, in future work we will re-design our models by replacing the exact  $E_c^{\text{MP2}}$  with some of its approximations.<sup>85–87</sup> The zero-cost size-consistency correction of Ref. 23 is an important part of our scheme and for now it can be applied only to systems dissociating into non-degenerate ground states. Generalization of this correction for systems that dissociate into degenerate ground state fragments will be another objective for future works. This and the investigation of the large-coupling limit of the MP AC for open-shell systems should pave the way for the broader applicability of our scheme (i.e. beyond NCIs). The development of analytical gradients enabling further applicability of our method will be then considered following the similar implementation of gradients for standard double hybrids.<sup>?</sup> Our scheme can also be used to give a formal justification and to improve recently introduced double-hybrid functionals that are applied to Hartree-Fock densities.<sup>79</sup>

## Computational details

All calculations have been performed using a modified version of the TURBOMOLE 7.1 package.<sup>88,89</sup> Computational details are the same as in Refs. 90,91. For all MP2 calculations we have employed aug-cc-pVQZ enhanced with additional basis functions detailed in Ref. 23. MP2 interaction energies for NCIs within this basis set are close to the MP2/CBS results.<sup>66</sup> From these MP2 calculations we extract all the quantities needed to construct our MP AC interpolation models (HF densities,  $E_x[\{\phi_i^{\text{HF}}\}]$ ,  $E_c^{\text{MP2}}$ ). The B3LYP-D3 results shown in Table 1 for the S22, CT7 DI6, S66, and L7 datasets have been taken from Refs. 34,36,77,77,92, respectively, whereas for NGD8 they were calculated using an aug-cc-pVQZ basis set. The same basis set has been employed to calculate MP3 and MP4 energies for Kr<sub>2</sub>. For B2PLYP-D3 the data for L7 was obtained from Ref 93. The B2PLYP, B3LYP-D3 and CCSD(T)/CBS data for the S66 dissociation curves were obtained from 69. The B2PLYP(-D3), B3LYP(-D3) and CCSD(T)/CBS data for the CT7 dissociation curves were calculated using an aug-cc-pVQZ basisset. The B3LYP-D3 for the dissociation curves of Ne<sub>2</sub>, Kr<sub>2</sub> and Ar<sub>2</sub> were obtained from 94, whereas the rest of the B3LYP-D3, B2PLYP and CCSD(T) data were again calculated with the basisset aug-cc-pVQZ.

For SPL2 the optimal parameters we find are ( $b_2 = 0.117$ ,  $m_2 = 10.68$ ,  $\alpha = 1.1472$ ,  $\beta = -0.7397$ ), whereas for MPACF-1 we use the following set of parameters, ( $d_1 = 0.294$ ,  $d_2 = 0.934$ ). A few remarks on these parameters are needed. As shown in Ref. 32, the large- $\lambda$  limit of the MP AC integrand  $W_{c,\lambda}$  has a leading term  $W_{c,\infty}$  which is much lower than its DFT counterpart. At the next order, the  $\lambda^{-1/2}$  term is, instead, positive and much larger than its DFT counterpart, because the HF exchange operator enhances the zero-point energy, by introducing excited states of the normal modes.<sup>32</sup> Finally, the  $\lambda^{-3/4}$  term is not present in the DFT AC, and it is a peculiar feature of the MP AC.<sup>32</sup> This term is again negative. Overall, these three terms together are needed for an accurate description of  $W_{c,\lambda}$ , as they balance each other in a delicate way (see Fig. 9 of Ref. 32). The SPL2 form does not have the  $\lambda^{-3/4}$  term. For this reason, its large- $\lambda$  limit  $W_{c,\infty}$  is an effective description of

the three leading terms; this is why in this case  $\beta$  turns out to be negative. In addition, we need to point out that the fitting procedure do not consider the total energies but takes into account only the interaction energies and should **only** be used within the SCC approach. The new MPACF-1 form, instead, has built in the correct large- $\lambda$  behavior, including the  $\lambda^{-3/4}$  term. This is why in this case the parameters  $\alpha$  and  $\beta$  can be set equal to 1. In future work we will build accurate GGA functionals for the first two leading terms of the large- $\lambda$  MP AC, which are expected to improve our models, when combined with an approximation for the  $\lambda^{-3/4}$  term containing the HF density at the nuclei. In Table S3 from the Supplementary Information,<sup>72</sup> we give a summary of the three MP AC forms, their parameters, etc., and highlight the differences in models for  $W_{c,\infty}$  that our three forms use.

## Supporting Information

The Supporting Information is available free of charge on the ACS Publications website ... at DOI: ...

- MAEs for S66 subsets, additional dissociation curves of noncovalent complexes, plots comparing errors for the L7 dataset, summary of MP AC forms developed in this work.

## Acknowledgments

Financial support by the Netherlands Organisation for Scientific Research under Vici grant 724.017.001 is acknowledged. This work was also supported the European Research Council under H2020/ERC Consolidator Grant corr-DFT (Grant No. 648932). SV acknowledges financial support from the Alexander von Humboldt Foundation.

## References

- (1) Hohenstein, E. G.; Sherrill, C. D. Wavefunction methods for noncovalent interactions. *WIREs Computational Molecular Science* **2012**, *2*, 304–326.
- (2) Riley, K. E.; Hobza, P. Noncovalent interactions in biochemistry. *WIREs Computational Molecular Science* **2011**, *1*, 3–17.
- (3) Lao, K. U.; Herbert, J. M. Accurate and Efficient Quantum Chemistry Calculations for Noncovalent Interactions in Many-Body Systems: The XSAPT Family of Methods. *The Journal of Physical Chemistry A* **2015**, *119*, 235–252.
- (4) Sedlak, R.; Janowski, T.; Pitoňák, M.; Řezáč, J.; Pulay, P.; Hobza, P. Accuracy of Quantum Chemical Methods for Large Noncovalent Complexes. *Journal of Chemical Theory and Computation* **2013**, *9*, 3364–3374.
- (5) Gráfová, L.; Pitoňák, M.; Řezáč, J.; Hobza, P. Comparative Study of Selected Wave Function and Density Functional Methods for Noncovalent Interaction Energy Calculations Using the Extended S22 Data Set. *Journal of Chemical Theory and Computation* **2010**, *6*, 2365–2376.
- (6) Al-Hamdani, Y. S.; Tkatchenko, A. Understanding non-covalent interactions in larger molecular complexes from first principles. *The Journal of Chemical Physics* **2019**, *150*, 010901.
- (7) Grimme, S.; Hansen, A.; Brandenburg, J. G.; Bannwarth, C. Dispersion-Corrected Mean-Field Electronic Structure Methods. *Chemical Reviews* **2016**, *116*, 5105–5154.
- (8) Dubecký, M.; Mitas, L.; Jurečka, P. Noncovalent Interactions by Quantum Monte Carlo. *Chemical Reviews* **2016**, *116*, 5188–5215.
- (9) Christensen, A. S.; Kubař, T.; Cui, Q.; Elstner, M. Semiempirical Quantum Mechani-

- cal Methods for Noncovalent Interactions for Chemical and Biochemical Applications. *Chemical Reviews* **2016**, *116*, 5301–5337.
- (10) Burns, L. A.; Mayagoitia, A. V.; Sumpter, B. G.; Sherrill, C. D. Density-functional approaches to noncovalent interactions: A comparison of dispersion corrections (DFT-D), exchange-hole dipole moment (XDM) theory, and specialized functionals. *The Journal of Chemical Physics* **2011**, *134*, 084107.
  - (11) DiLabio, G. A.; Johnson, E. R.; Otero-de-la Roza, A. Performance of conventional and dispersion-corrected density-functional theory methods for hydrogen bonding interaction energies. *Phys. Chem. Chem. Phys.* **2013**, *15*, 12821–12828.
  - (12) Grimme, S.; Antony, J.; Ehrlich, S.; Krieg, H. A consistent and accurate ab initio parametrization of density functional dispersion correction (DFT-D) for the 94 elements H-Pu. *The Journal of Chemical Physics* **2010**, *132*, 154104.
  - (13) Hobza, P. The calculation of intermolecular interaction energies. *Annu. Rep. Prog. Chem., Sect. C: Phys. Chem.* **2011**, *107*, 148–168.
  - (14) Laricchia, S.; Fabiano, E.; Della Sala, F. On the accuracy of frozen density embedding calculations with hybrid and orbital-dependent functionals for non-bonded interaction energies. *The Journal of Chemical Physics* **2012**, *137*, 014102.
  - (15) Grabowski, I.; Fabiano, E.; Della Sala, F. A simple non-empirical procedure for spin-component-scaled MP2 methods applied to the calculation of the dissociation energy curve of noncovalently-interacting systems. *Phys. Chem. Chem. Phys.* **2013**, *15*, 15485–15493.
  - (16) Fabiano, E.; Constantin, L. A.; Della Sala, F. Wave Function and Density Functional Theory Studies of Dihydrogen Complexes. *Journal of Chemical Theory and Computation* **2014**, *10*, 3151–3162.

- (17) Fabiano, E.; Della Sala, F.; Grabowski, I. Accurate non-covalent interaction energies via an efficient MP2 scaling procedure. *Chemical Physics Letters* **2015**, *635*, 262–267.
- (18) Śmiga, S.; Fabiano, E. Approximate solution of coupled cluster equations: application to the coupled cluster doubles method and non-covalent interacting systems. *Phys. Chem. Chem. Phys.* **2017**, *19*, 30249–30260.
- (19) Fabiano, E.; Cortona, P. Dispersion corrections applied to the TCA family of exchange-correlation functionals. *Theor Chem Acc* **2017**, *136*, 88.
- (20) Riley, K. E.; Platts, J. A.; Řezáč, J.; Hobza, P.; Hill, J. G. Assessment of the Performance of MP2 and MP2 Variants for the Treatment of Noncovalent Interactions. *The Journal of Physical Chemistry A* **2012**, *116*, 4159–4169.
- (21) Hobza, P.; Zahradnik, R. Intermolecular interactions between medium-sized systems. Nonempirical and empirical calculations of interaction energies. Successes and failures. *Chemical Reviews* **1988**, *88*, 871–897.
- (22) Nguyen, B. D.; Chen, G. P.; Agee, M. M.; Burow, A. M.; Tang, M. P.; Furche, F. Divergence of Many-Body Perturbation Theory for Noncovalent Interactions of Large Molecules. *Journal of Chemical Theory and Computation* **2020**, *16*, 2258–2273.
- (23) Vuckovic, S.; Gori-Giorgi, P.; Della Sala, F.; Fabiano, E. Restoring size consistency of approximate functionals constructed from the adiabatic connection. *J. Phys. Chem. Lett.* **2018**, *9*, 3137–3142.
- (24) Grimme, S. Semiempirical hybrid density functional with perturbative second-order correlation. *The Journal of Chemical Physics* **2006**, *124*, 034108.
- (25) Schwabe, T.; Grimme, S. Double-hybrid density functionals with long-range dispersion corrections: higher accuracy and extended applicability. *Phys. Chem. Chem. Phys.* **2007**, *9*, 3397–3406.

- (26) Caldeweyher, E.; Ehlert, S.; Hansen, A.; Neugebauer, H.; Spicher, S.; Bannwarth, C.; Grimme, S. A generally applicable atomic-charge dependent London dispersion correction. *The Journal of Chemical Physics* **2019**, *150*, 154122.
- (27) Caldeweyher, E.; Mewes, J.-M.; Ehlert, S.; Grimme, S. Extension and evaluation of the D4 London-dispersion model for periodic systems. *Phys. Chem. Chem. Phys.* **2020**, *22*, 8499–8512.
- (28) Zhang, Y.; Xu, X.; Goddard, W. A. Doubly hybrid density functional for accurate descriptions of nonbond interactions, thermochemistry, and thermochemical kinetics. *Proceedings of the National Academy of Sciences* **2009**, *106*, 4963–4968.
- (29) Zhang, I. Y.; Xu, X. Exploring the Limits of the XYG3-Type Doubly Hybrid Approximations for the Main-Group Chemistry: The xDH@B3LYP Model. *The Journal of Physical Chemistry Letters* **2021**, *12*, 2638–2644.
- (30) Santra, G.; Sylvetsky, N.; Martin, J. M. L. Minimally Empirical Double-Hybrid Functionals Trained against the GMTKN55 Database: revDSD-PBEP86-D4, revDOD-PBE-D4, and DOD-SCAN-D4. *The Journal of Physical Chemistry A* **2019**, *123*, 5129–5143.
- (31) Seidl, M.; Giarrusso, S.; Vuckovic, S.; Fabiano, E.; Gori-Giorgi, P. Communication: Strong-interaction limit of an adiabatic connection in Hartree-Fock theory. *The Journal of Chemical Physics* **2018**, *149*, 241101.
- (32) Daas, T. J.; Grossi, J.; Vuckovic, S.; Musslimani, Z. H.; Kooi, D. P.; Seidl, M.; Giesbertz, K. J. H.; Gori-Giorgi, P. Large coupling-strength expansion of the Møller–Plesset adiabatic connection: From paradigmatic cases to variational expressions for the leading terms. *The Journal of Chemical Physics* **2020**, *153*, 214112.
- (33) Seidl, M.; Perdew, J. P.; Levy, M. Strictly correlated electrons in density-functional theory. *Phys. Rev. A* **1999**, *59*, 51–54.

- (34) Sedlak, R.; Janowski, T.; Pitoňák, M.; Řezáč, J.; Pulay, P.; Hobza, P. Accuracy of Quantum Chemical Methods for Large Noncovalent Complexes. *Journal of Chemical Theory and Computation* **2013**, *9*, 3364–3374.
- (35) Al-Hamdani, Y. S.; Nagy, P. R.; Barton, D.; Kállay, M.; Brandenburg, J. G.; Tkatchenko, A. Interactions between Large Molecules: Puzzle for Reference Quantum-Mechanical Methods. 2020.
- (36) Grimme, S.; Brandenburg, J. G.; Bannwarth, C.; Hansen, A. Consistent structures and interactions by density functional theory with small atomic orbital basis sets. *The Journal of Chemical Physics* **2015**, *143*, 054107.
- (37) Tkatchenko, A.; Scheffler, M. Accurate Molecular Van Der Waals Interactions from Ground-State Electron Density and Free-Atom Reference Data. *Phys. Rev. Lett.* **2009**, *102*, 073005.
- (38) Pernal, K. Correlation energy from random phase approximations: A reduced density matrices perspective. *Int. J. Quantum. Chem.* **2018**, *118*, e25462.
- (39) Marie, A.; Burton, H. G. A.; Loos, P.-F. Perturbation Theory in the Complex Plane: Exceptional Points and Where to Find Them. *Journal of Physics: Condensed Matter* **2021**,
- (40) Möller, C.; Plesset, M. S. Note on an Approximation Treatment for Many-Electron Systems. *Phys. Rev.* **1934**, *46*, 618–622.
- (41) Seidl, M.; Gori-Giorgi, P.; Savin, A. Strictly correlated electrons in density-functional theory: A general formulation with applications to spherical densities. *Phys. Rev. A* **2007**, *75*, 042511/12.
- (42) Gori-Giorgi, P.; Vignale, G.; Seidl, M. Electronic Zero-Point Oscillations in the Strong-



- Interaction Limit of Density Functional Theory. *J. Chem. Theory Comput.* **2009**, *5*, 743–753.
- (43) Langreth, D. C.; Perdew, J. P. The exchange-correlation energy of a metallic surface. *Solid. State Commun.* **1975**, *17*, 1425–1429.
- (44) Gunnarsson, O.; Lundqvist, B. I. Exchange and correlation in atoms, molecules, and solids by the spin-density-functional formalism. *Phys. Rev. B* **1976**, *13*, 4274–4298.
- (45) Gori-Giorgi, P.; Seidl, M.; Savin, A. *Phys. Chem. Chem. Phys.* **2008**, *10*, 3440.
- (46) Gori-Giorgi, P.; Seidl, M.; Vignale, G. Density-Functional Theory for Strongly Interacting Electrons. *Phys. Rev. Lett.* **2009**, *103*, 166402.
- (47) Grossi, J.; Kooi, D. P.; Giesbertz, K. J. H.; Seidl, M.; Cohen, A. J.; Mori-Sánchez, P.; Gori-Giorgi, P. Fermionic statistics in the strongly correlated limit of Density Functional Theory. *J. Chem. Theory Comput.* **2017**, *13*, 6089–6100.
- (48) Görling, A.; Levy, M. *Phys. Rev. B* **1993**, *47*, 13105.
- (49) Görling, A.; Levy, M. Exact Kohn-Sham scheme based on perturbation theory. *Phys. Rev. A* **1994**, *50*, 196.
- (50) Seidl, M.; Perdew, J. P.; Kurth, S. *Phys. Rev. A* **2000**, *62*, 012502.
- (51) Wagner, L. O.; Gori-Giorgi, P. Electron avoidance: A nonlocal radius for strong correlation. *Phys. Rev. A* **2014**, *90*, 052512.
- (52) Bahmann, H.; Zhou, Y.; Ernzerhof, M. The shell model for the exchange-correlation hole in the strong-correlation limit. *J. Chem. Phys.* **2016**, *145*, 124104.
- (53) Vuckovic, S.; Gori-Giorgi, P. Simple Fully Nonlocal Density Functionals for Electronic Repulsion Energy. *The Journal of Physical Chemistry Letters* **2017**, *8*, 2799–2805.

- (54) Gould, T.; Vuckovic, S. Range-separation and the multiple radii functional approximation inspired by the strongly interacting limit of density functional theory. *The Journal of Chemical Physics* **2019**, *151*, 184101.
- (55) Becke, A. D. A new mixing of Hartree–Fock and local density-functional theories. *J. Chem. Phys.* **1993**, *98*, 1372.
- (56) Becke, A. D. Density-functional thermochemistry. III. The role of exact exchange. *J. Chem. Phys.* **1993**, *98*, 5648.
- (57) Perdew, J. P.; Ernzerhof, M.; Burke, K. Rationale for mixing exact exchange with density functional approximations. *J. Chem. Phys.* **1996**, *105*, 9982–9985.
- (58) Sharkas, K.; Toulouse, J.; Savin, A. *J. Chem. Phys.* **2011**, *134*, 064113.
- (59) Goerigk, L.; Grimme, S. Efficient and Accurate Double-Hybrid-Meta-GGA Density Functionals Evaluation with the Extended GMTKN30 Database for General Main Group Thermochemistry, Kinetics, and Noncovalent Interactions. *J. Chem. Theory Comput.* **2010**, *7*, 291–309.
- (60) Su, N. Q.; Xu, X. Construction of a parameter-free doubly hybrid density functional from adiabatic connection. *J. Chem. Phys.* **2014**, *140*, 18A512.
- (61) Vuckovic, S.; Irons, T. J. P.; Savin, A.; Teale, A. M.; Gori-Giorgi, P. Exchange–correlation functionals via local interpolation along the adiabatic connection. *J. Chem. Theory Comput.* **2016**, *12*, 2598–2610.
- (62) Pastorczak, E.; Hapka, M.; Veis, L.; Pernal, K. Capturing the Dynamic Correlation for Arbitrary Spin-Symmetry CASSCF Reference with Adiabatic Connection Approaches: Insights into the Electronic Structure of the Tetramethyleneethane Diradical. *The Journal of Physical Chemistry Letters* **2019**, *10*, 4668–4674.

- (63) Maradzike, E.; Hapka, M.; Pernal, K.; DePrince, A. E. Reduced Density Matrix-Driven Complete Active Space Self-Consistent Field Corrected for Dynamic Correlation from the Adiabatic Connection. *Journal of Chemical Theory and Computation* **2020**, *16*, 4351–4360.
- (64) Seidl, M.; Perdew, J. P.; Kurth, S. Simulation of All-Order Density-Functional Perturbation Theory, Using the Second Order and the Strong-Correlation Limit. *Phys. Rev. Lett.* **2000**, *84*, 5070–5073.
- (65) Vuckovic, S.; Irons, T. J. P.; Wagner, L. O.; Teale, A. M.; Gori-Giorgi, P. Interpolated energy densities, correlation indicators and lower bounds from approximations to the strong coupling limit of DFT. *Phys. Chem. Chem. Phys.* **2017**, *19*, 6169–6183.
- (66) Vuckovic, S.; Fabiano, E.; Gori-Giorgi, P.; Burke, K. MAP: An MP2 Accuracy Predictor for Weak Interactions from Adiabatic Connection Theory. *Journal of Chemical Theory and Computation* **2020**, *16*, 4141–4149.
- (67) Constantin, L. A. Correlation energy functionals from adiabatic connection formalism. *Phys. Rev. B* **2019**, *99*, 085117.
- (68) Mirtschink, A.; Seidl, M.; Gori-Giorgi, P. Energy densities in the strong-interaction limit of density functional theory. *J. Chem. Theory Comput.* **2012**, *8*, 3097–3107.
- (69) Řezáč, J.; Riley, K. E.; Hobza, P. S66: A Well-balanced Database of Benchmark Interaction Energies Relevant to Biomolecular Structures. *Journal of Chemical Theory and Computation* **2011**, *7*, 2427–2438.
- (70) Jurečka, P.; Šponer, J.; Černý, J.; Hobza, P. Benchmark database of accurate (MP2 and CCSD(T) complete basis set limit) interaction energies of small model complexes, DNA base pairs, and amino acid pairs. *Phys. Chem. Chem. Phys.* **2006**, *8*, 1985–1993.

- (71) Takatani, T.; Hohenstein, E. G.; Malagoli, M.; Marshall, M. S.; Sherrill, C. D. Basis set consistent revision of the S22 test set of noncovalent interaction energies. *The Journal of chemical physics* **2010**, *132*, 144104.
- (72) See Supplemental information at .... for further information, figures and tables.
- (73) Vuckovic, S.; Burke, K. Quantifying and Understanding Errors in Molecular Geometries. *The Journal of Physical Chemistry Letters* **2020**, *11*, 9957–9964.
- (74) Zhao, Y.; Truhlar, D. G. Benchmark Databases for Nonbonded Interactions and Their Use To Test Density Functional Theory. *Journal of Chemical Theory and Computation* **2005**, *1*, 415–432.
- (75) Zhao, Y.; Schultz, N. E.; Truhlar, D. G. Exchange-correlation functional with broad accuracy for metallic and nonmetallic compounds, kinetics, and noncovalent interactions. *The Journal of Chemical Physics* **2005**, *123*, 161103.
- (76) Zhao, Y.; Schultz, N. E.; Truhlar, D. G. *J. Chem. Theory Comput.* **2006**, *2*, 364.
- (77) Zhang, I. Y.; Xu, X.; Jung, Y.; Goddard, W. A. A fast doubly hybrid density functional method close to chemical accuracy using a local opposite spin ansatz. *Proceedings of the National Academy of Sciences* **2011**, *108*, 19896–19900.
- (78) Kim, Y.; Song, S.; Sim, E.; Burke, K. Halogen and Chalcogen Binding Dominated by Density-Driven Errors. *The Journal of Physical Chemistry Letters* **2018**, *10*, 295–301.
- (79) Song, S.; Vuckovic, S.; Sim, E.; Burke, K. Density Sensitivity of Empirical Functionals. *The Journal of Physical Chemistry Letters* **2021**, *12*, 800–807.
- (80) Mehta, N.; Fellowes, T.; WHITE, J.; Goerigk, L. TheCHAL336 Benchmark Set: How Well Do Quantum-Chemical Methods Describe Chalcogen-Bonding Interactions? **2021**,

- (81) Mardirossian, N.; Head-Gordon, M.  $\omega$ B97M-V: A combinatorially optimized, range-separated hybrid, meta-GGA density functional with VV10 nonlocal correlation. *The Journal of Chemical Physics* **2016**, *144*, 214110.
- (82) Mardirossian, N.; Head-Gordon, M. Thirty years of density functional theory in computational chemistry: an overview and extensive assessment of 200 density functionals. *Molecular Physics* **2017**, *115*, 2315–2372.
- (83) Mardirossian, N.; Head-Gordon, M. Survival of the most transferable at the top of Jacob’s ladder: Defining and testing the  $\omega$ B97M(2) double hybrid density functional. *The Journal of Chemical Physics* **2018**, *148*, 241736.
- (84) McGibbon, R. T.; Taube, A. G.; Donchev, A. G.; Siva, K.; Hernández, F.; Hargus, C.; Law, K.-H.; Klepeis, J. L.; Shaw, D. E. Improving the accuracy of Møller-Plesset perturbation theory with neural networks. *The Journal of Chemical Physics* **2017**, *147*, 161725.
- (85) Schütz, M.; Hetzer, G.; Werner, H.-J. Low-order scaling local electron correlation methods. I. Linear scaling local MP2. *The Journal of Chemical Physics* **1999**, *111*, 5691–5705.
- (86) Lee, M. S.; Maslen, P. E.; Head-Gordon, M. Closely approximating second-order Møller–Plesset perturbation theory with a local triatomics in molecules model. *The Journal of Chemical Physics* **2000**, *112*, 3592–3601.
- (87) Williams, Z. M.; Wiles, T. C.; Manby, F. R. Accurate Hybrid Density Functionals with UW12 Correlation. *Journal of Chemical Theory and Computation* **2020**, *16*, 6176–6194.
- (88) Furche, F.; Ahlrichs, R.; Hättig, C.; Klopper, W.; Sierka, M.; Weigend, F. Turbomole. *WIREs Computational Molecular Science* **2014**, *4*, 91–100.

- (89) TURBOMOLE V7.1 2010, a development of University of Karlsruhe and Forschungszentrum Karlsruhe GmbH, 1989-2007, TURBOMOLE GmbH, since 2007; available from <http://www.turbomole.com>.
- (90) Fabiano, E.; Gori-Giorgi, P.; Seidl, M.; Della Sala, F. Interaction-Strength Interpolation Method for Main-Group Chemistry: Benchmarking, Limitations, and Perspectives. *J. Chem. Theory. Comput.* **2016**, *12*, 4885–4896.
- (91) Giarrusso, S.; Gori-Giorgi, P.; Della Sala, F.; Fabiano, E. Assessment of interaction-strength interpolation formulas for gold and silver clusters. *J. Chem. Phys.* **2018**, *148*, 134106.
- (92) Goerigk, L.; Hansen, A.; Bauer, C.; Ehrlich, S.; Najibi, A.; Grimme, S. A look at the density functional theory zoo with the advanced GMTKN55 database for general main group thermochemistry, kinetics and noncovalent interactions. *Physical Chemistry Chemical Physics* **2017**, *19*, 32184–32215.
- (93) Calbo, J.; Ortí, E.; Sancho-García, J. C.; Aragó, J. Accurate Treatment of Large Supramolecular Complexes by Double-Hybrid Density Functionals Coupled with Non-local van der Waals Corrections. *Journal of Chemical Theory and Computation* **2015**, *11*, 932–939.
- (94) Kovács, A.; Cz. Dobrowolski, J.; Ostrowski, S.; Rode, J. E. Benchmarking density functionals in conjunction with Grimme’s dispersion correction for noble gas dimers (Ne<sub>2</sub>, Ar<sub>2</sub>, Kr<sub>2</sub>, Xe<sub>2</sub>, Rn<sub>2</sub>). *International Journal of Quantum Chemistry* **2017**, *117*, e25358.

*Supporting Information for*

**“Noncovalent interactions from models for the  
Møller-Plesset adiabatic connection”**

Timothy J. Daas,<sup>†</sup> Eduardo Fabiano,<sup>‡,P</sup> Fabio Della Sala,<sup>‡,P</sup> Paola Gori-Giorgi,<sup>†</sup>  
and Stefan Vuckovic<sup>\*,§,||,†</sup>

<sup>†</sup>*Department of Chemistry & Pharmaceutical Sciences and Amsterdam Institute of  
Molecular and Life Sciences (AIMMS), Faculty of Science, Vrije Universiteit, De Boelelaan  
1083, 1081HV Amsterdam, The Netherlands*

<sup>‡</sup>*Institute for Microelectronics and Microsystems (CNR-IMM), Via Monteroni, Campus  
Unisalento, 73100 Lecce, Italy*

<sup>P</sup>*Center for Biomolecular Nanotechnologies, Istituto Italiano di Tecnologia, Via Barsanti  
14, 73010 Arnesano (LE), Italy*

<sup>§</sup>*Physical and Theoretical Chemistry, University of Saarland, 66123 Saarbrücken, Germany*

<sup>||</sup>*Department of Chemistry, University of California, Irvine, CA 92697, USA*

E-mail: svuckovi@uci.edu

**Table S1:** MAEs in kcal/mol of MP2, SPL, MPACF-1 and SPL2 for the three subsets of the S66 dataset.

method	H-bonds	dispersion	others
MP2	0.18	0.82	0.41
SPL	0.42	0.42	0.19
MPACF-1	0.15	0.45	0.17
SPL2	0.19	0.30	0.12

**Table S2:** MAEs of 3 different reference calculations relative to each other, as well as the MAEs of MP2, SPL, SPL2, MPACF-1 relative to each of the three references for the L7 dataset. Regardless of the reference, SPL gives improvement over MP2 and SPL2 and MPACF-1 give improvements over SPL. Data from ref. 1 for L7 were obtained from DLPNO-CCSD(T) and a newly developed CBS extrapolation scheme,<sup>?</sup> ref. 2 using QCISD(T)/CBS<sup>?</sup> and ref. 3 using LNO-CCSD(T)/CBS(Q,5)) (Local Natural Orbital).<sup>?</sup> We used ref. 1 of Grimme and co-workers in the main paper. For interaction energies of individual complexes, see Fig. S2

MAE	ref. 1	ref. 2	ref. 3
ref. 1	0	1.70	0.77
ref. 2	1.70	0	1.36
ref. 3	0.77	1.36	0
MP2	8.74	7.20	8.55
SPL	3.83	2.59	3.74
SPL2	0.89	1.26	0.95
MPACF-1	2.32	1.50	2.42



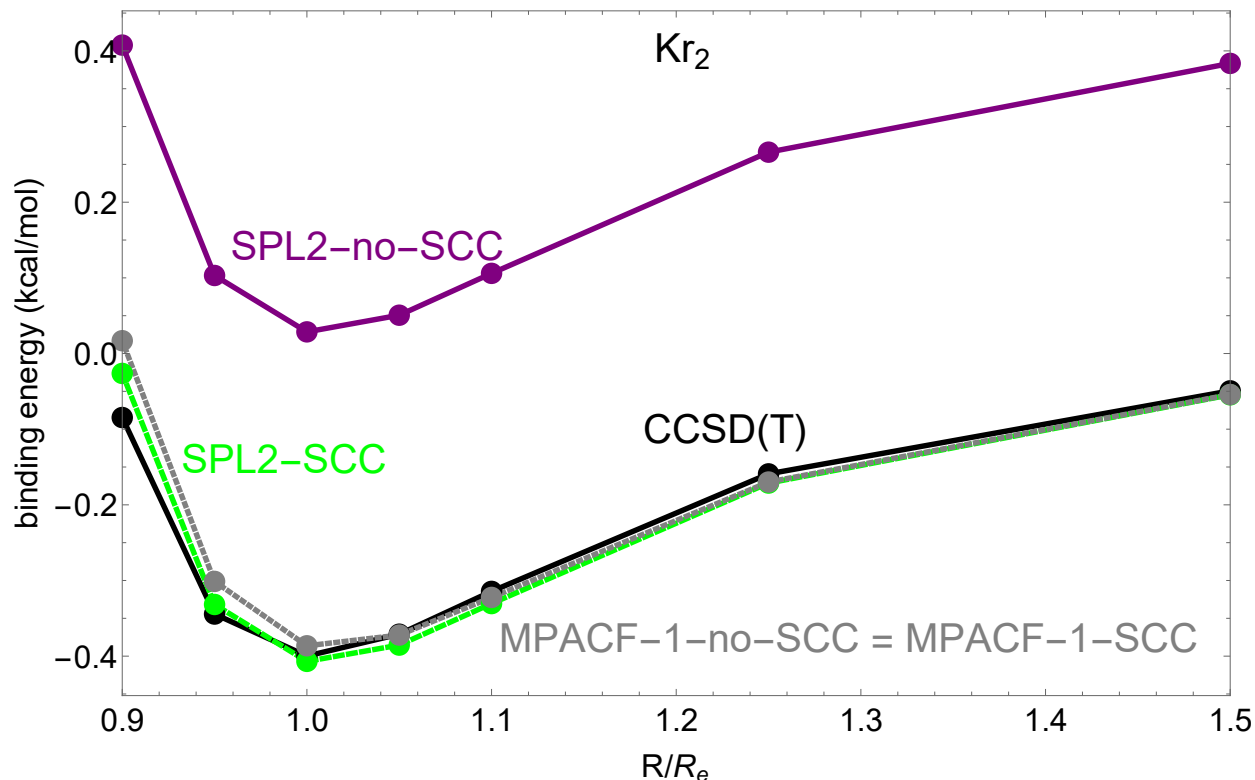


Figure S1: The SPL2 with and without size consistency corrections (SCC) plotted for the  $\text{Kr}_2$  vs the MPACF-1 method with and without SSC and the reference CCSD(T) data. For a complex composed by identical fragments  $A$ , the following equation,  $W^{\text{model}}(N\mathbf{W}(A)) = NW^{\text{model}}(\mathbf{W}(A))$ , is a size-extensivity requirement for adiabatic connection model functions,  $W^{\text{model}}$ , with  $\mathbf{W}(A) = \{W_1(A), \dots, W_i(A)\}$  being a compact notation for the  $i$  input ingredients for fragment  $A$  and  $N$  the number of fragments.<sup>?</sup> SPL2 violates this equation, while MPACF-1 obeys it. Because of that, without the SCC, interaction energies of SPL2 do not vanish even for systems that dissociate into equal fragments as it can be seen from the  $\text{Kr}_2$  example here. Since MPACF-1 is size-extensive, the addition of the SCC does not change the  $\text{Kr}_2$  dissociation curve, as it is already correct in the dissociation limit. In any case, all our models must be used with the SCC as it ensures that the interaction energies vanish in the dissociation limits (at least for systems dissociating into fragments with non-degenerate ground-state). Without the SCC, meaningless interaction energies would be obtained in some instances [see Ref. ? ].

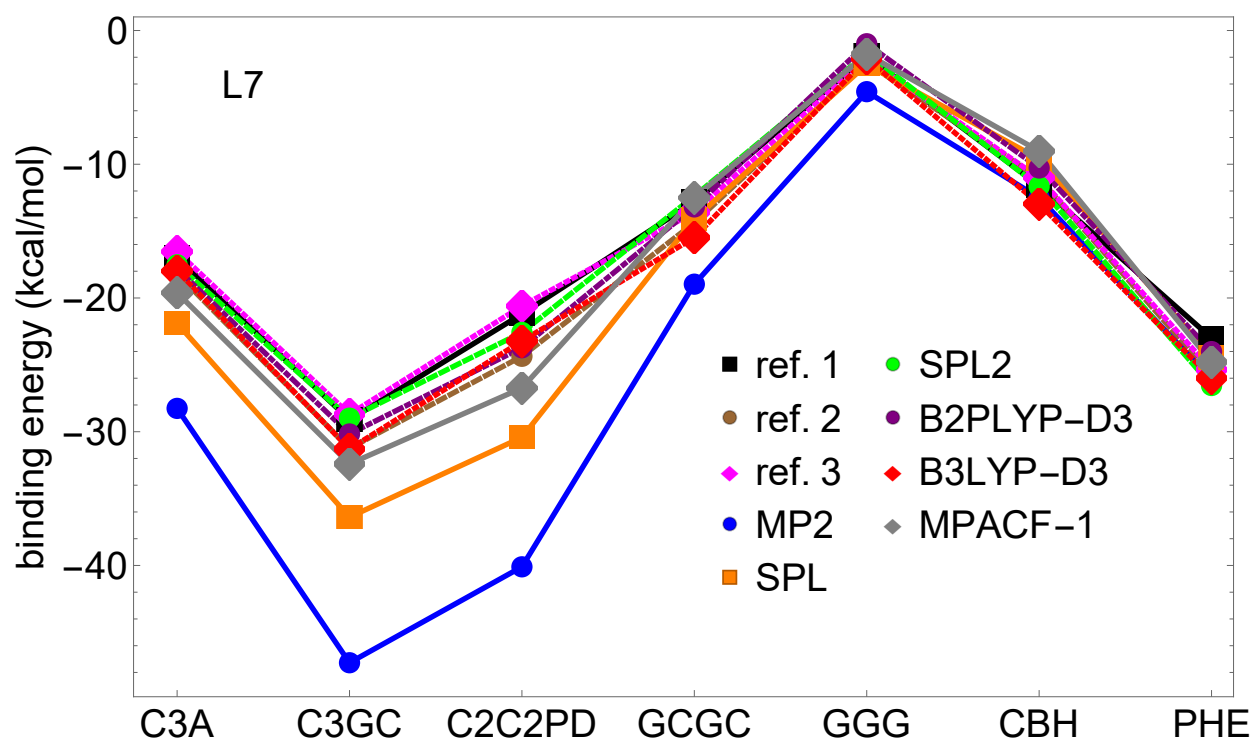


Figure S2: Interaction energies of MP2, SPL, SPL2, B3LYP-D3 and B2PLYP as well as three different reference (ref. 1 is Grimme et al.,<sup>?</sup> ref. 2 is Sedlak et al.<sup>?</sup> and ref. 3 is Al-Hamdani et al.<sup>?</sup>) data plotted for all 7 complexes of the L7 dataset. For further details on these references, see Table S1.

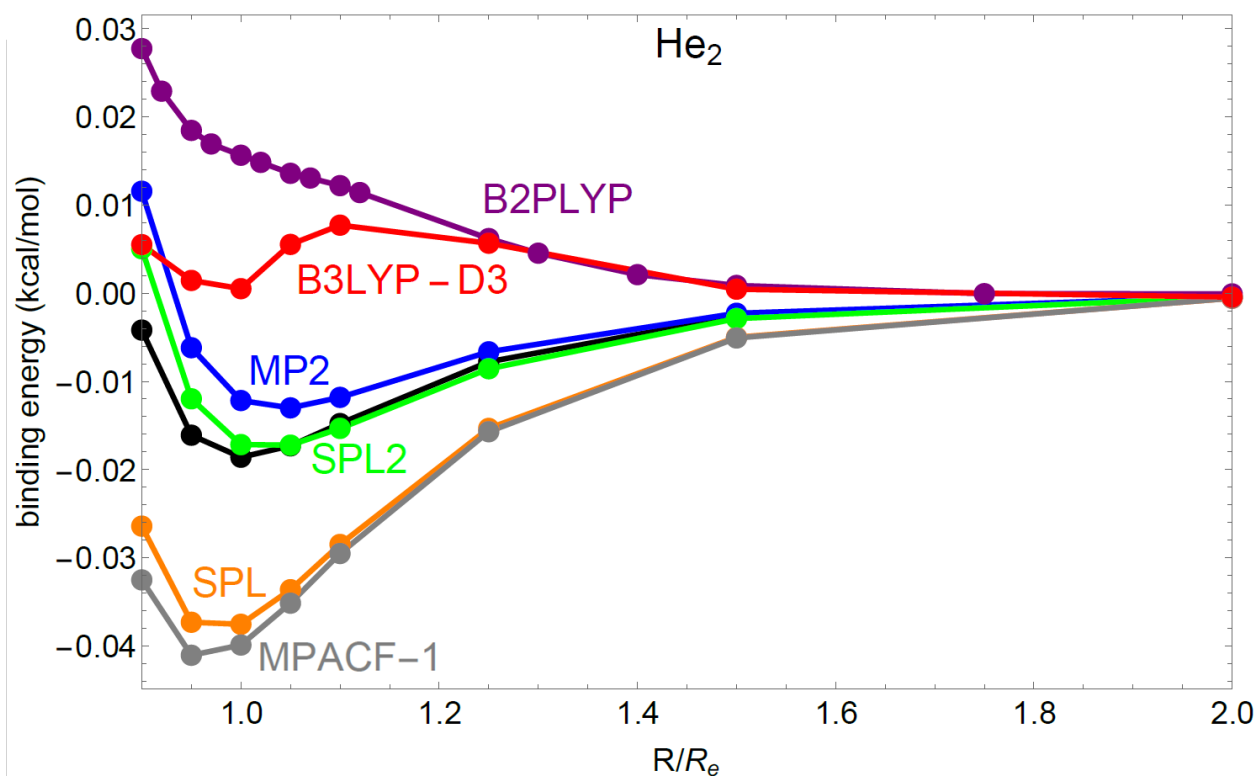


Figure S3: The interaction energies of MP2, SPL, SPL2, MPACF-1, B3LYP-D3 and B2PLYP as well as reference CCSD(T) curves for  $\text{He}_2$ . B3LYP even upon addition of D3 is producing an unphysical curve.

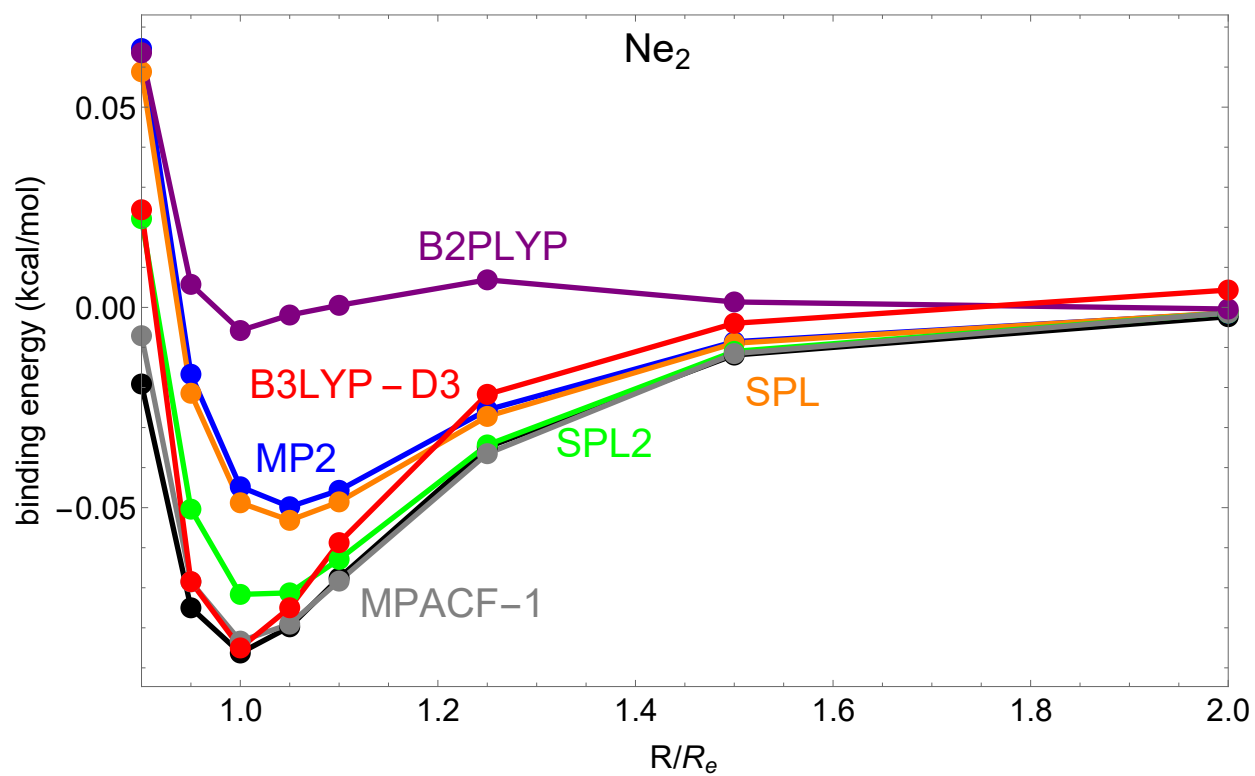


Figure S4: The interaction energies of MP2, SPL, SPL2, MPACF-1, B3LYP-D3 and B2PLYP as well as reference CCSD(T) curves for Ne<sub>2</sub>.

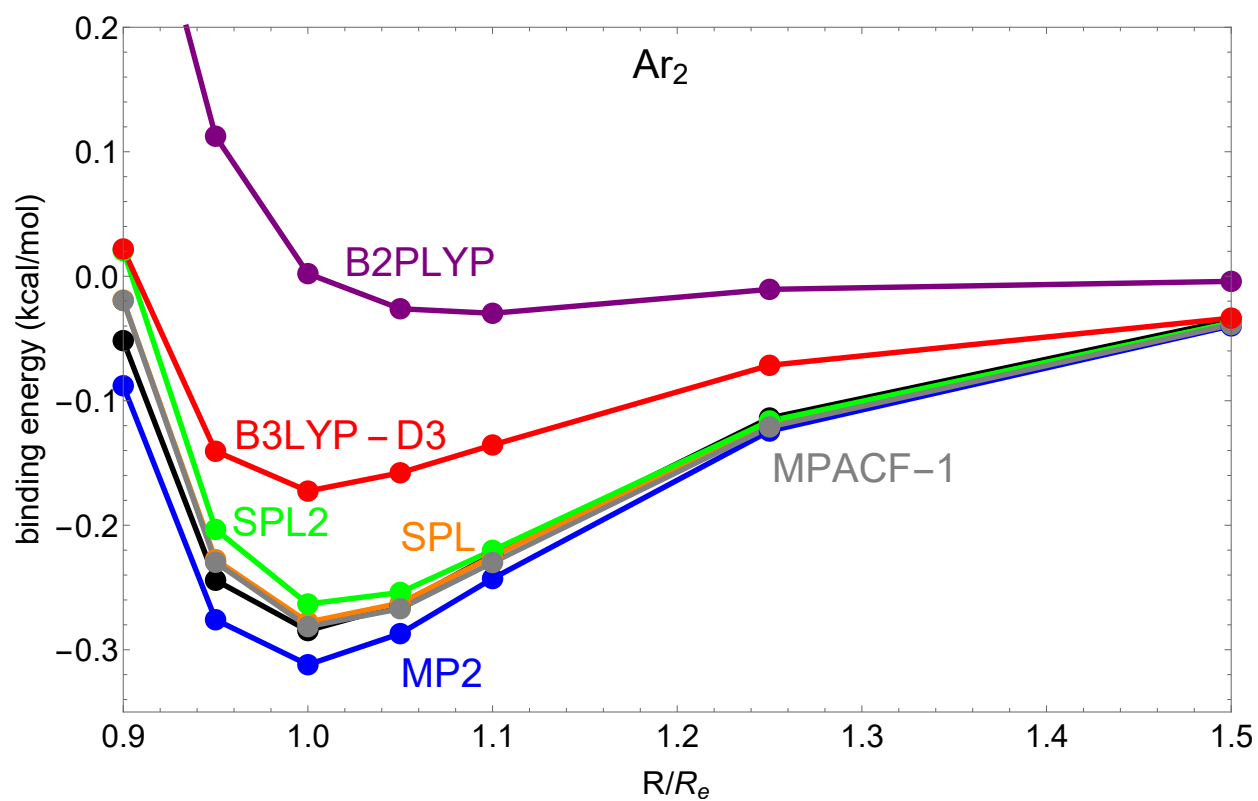


Figure S5: The interaction energies of MP2, SPL, SPL2, MPACF-1, B3LYP-D3 and B2PLYP as well as reference CCSD(T) curves for  $\text{Ar}_2$ .

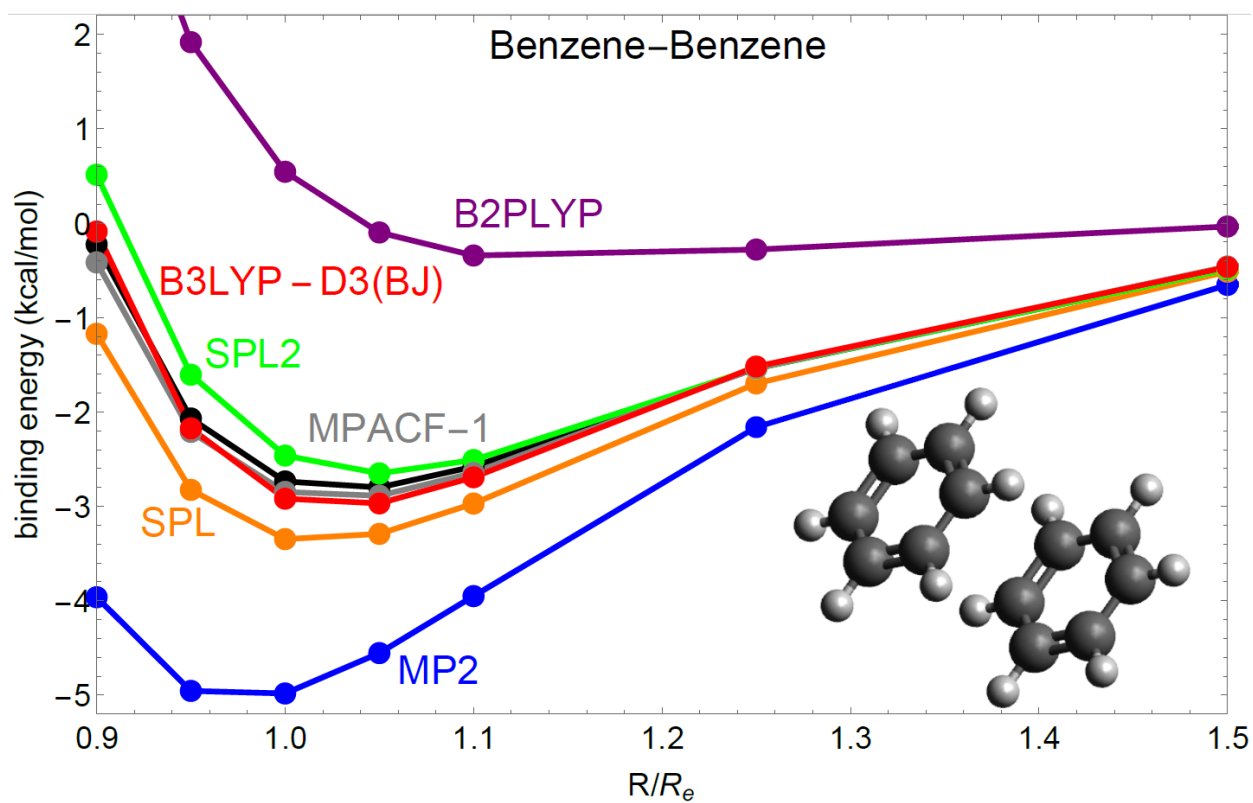


Figure S6: The interaction energies of MP2, SPL, SPL2, MPACF-1, B3LYP-D3(BJ) and B2PLYP as well as reference CCSD(T) curves for Benzene dimer.

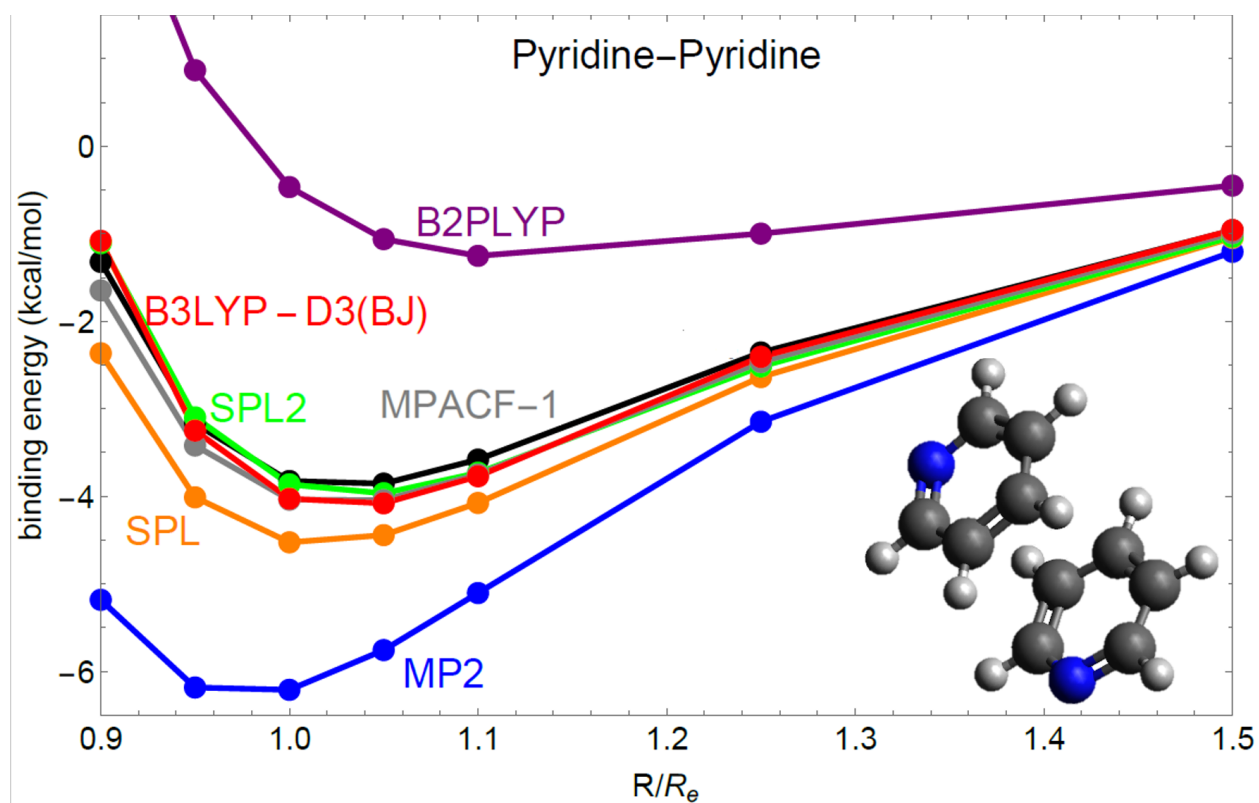


Figure S7: The interaction energies of MP2, SPL, SPL2, MPACF-1, B3LYP-D3(BJ) and B2PLYP as well as reference CCSD(T) curves for Pyridine dimer.

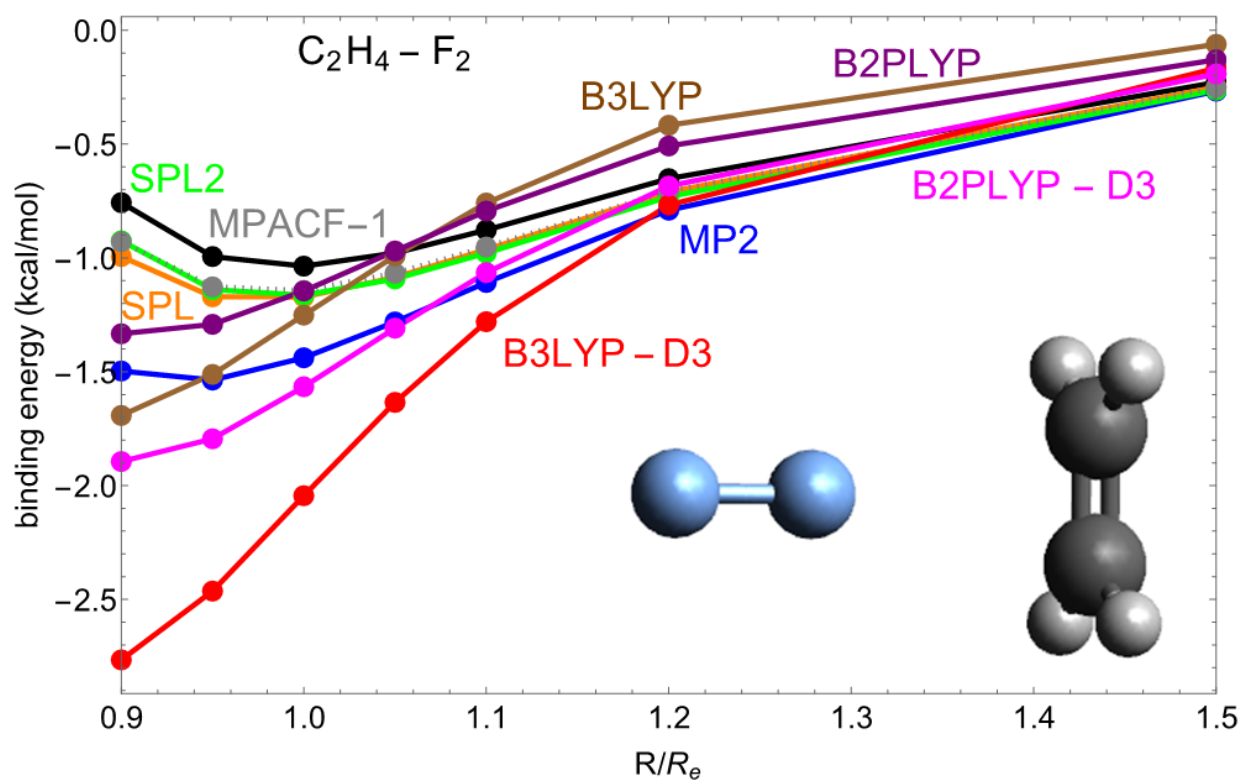


Figure S8: The interaction energies of MP2, SPL, SPL2, MPACF-1, B3LYP-D3 and B2PLYP as well as reference CCSD(T) curves for  $C_2H_4-F_2$



Table S3: The  $W_{c,\lambda}$  and  $E_c$  forms of the three different methods (SPL, SPL2 and MPACF-1) as well as their fixed and empirical parameters. For all forms,  $E_x$  and  $E_c^{MP2}$  are the exact exchange energy and the MP2 correlation energy respectively, whereas  $W_\infty^{PC}[\rho^{HF}]$  is a GEA functional ('PC model') evaluated on the HF density, which takes the following integral form:  $W_\infty^{PC}[\rho^{HF}] = \int \left[ A \rho^{HF}(\mathbf{r})^{4/3} + B \frac{|\nabla \rho^{HF}(\mathbf{r})|^2}{\rho^{HF}(\mathbf{r})^{4/3}} \right] d\mathbf{r}$  with  $A = -1.451$  and  $B = 5.317 \times 10^{-3}$ . In SPL,  $W_{c,\infty}$  form results from the PC model approximation to  $W_{c,\infty}^{DFT}$  as done in Ref. ? . In SPL2,  $W_{c,\infty}$  has been approximated in terms of the form containing  $\alpha$  and  $\beta$  parameters, which have been determined empirically. The form of  $W_{c,\infty}$  in MPACF-1 has been fixed by the large  $\lambda$  limit of the MP AC for the uniform electron gas.

	SPL	SPL2	MPACF-1
$W_{c,\lambda}$	$W_{c,\infty} \left( 1 - \frac{1}{\sqrt{1+b\lambda}} \right)$	$C_1 - \frac{m_1}{\sqrt{1+b_1\lambda}} - \frac{m_2}{\sqrt{1+b_2\lambda}}$	$g \left( \frac{(h+1) \left( h \sqrt{d_1^2\lambda+1} (3d_2^3\lambda+4) + 2(d_1^2\lambda+2)(d_2^3\lambda+1)^{3/4} \right)}{4\sqrt{d_1^2\lambda+1}(d_2^3\lambda+1)^{3/4}} \left( \sqrt{d_1^2\lambda+1} + h \sqrt[4]{d_2^3\lambda+1} \right)^2 - 1 \right)$
$E_c = \int_0^1 W_{c,\lambda} d\lambda$	$W_{c,\infty} \left( \frac{2+b-2\sqrt{1+b}}{b} \right)$	$C_1 - \frac{2m_1(\sqrt{1+b_1}-1)}{b_1} - \frac{2m_2(\sqrt{1+b_2}-1)}{b_2}$	$-g + \frac{g(h+1)}{\sqrt{d_1^2+1} + h \sqrt[4]{d_2^3+1}}$
$W_{c,\infty}$	$W_\infty^{PC}[\rho^{HF}] - E_x$	$\alpha W_\infty^{PC}[\rho^{HF}] + \beta E_x$	$\alpha W_\infty^{PC}[\rho^{HF}] + \beta E_x$
Fixed params.	$b = \frac{4E_c^{MP2}}{W_{c,\infty}}$	$C_1 = W_{c,\infty}, b_1 = \frac{b_2}{m_2 - 4E_c^{MP2}}, m_1 = W_{c,\infty} - m_2$	$g = -W_{c,\infty}, h = \frac{4E_c^{MP2} - 2d_1^2 W_{c,\infty}}{-4E_c^{MP2} + d_2^4 W_{c,\infty}}$
Emp. params.	-	$b_2 = 0.117, m_2 = 10.68, \alpha = 1.1472, \beta = -0.7397$	$d_1 = 0.294, d_2 = 0.934, \alpha = 1, \beta = 1$